Hindawi
Journal of Chemistry
Volume 2017, Article ID 1489218, 20 pages
https://doi.org/10.1155/2017/1489218

Research Article

Active Razor Shell CaO Catalyst Synthesis for Jatropha Methyl Ester Production via Optimized Two-Step Transesterification

A. N. R. Reddy,[1] A. A. Saleh,[1] M. S. Islam,[2] and S. Hamdan[1]

[1]*Department of Mechanical and Manufacturing Engineering, Faculty of Engineering, Universiti Malaysia Sarawak, 94300 Kota Samarahan, Sarawak, Malaysia*
[2]*Department of Chemistry, Bangladesh Army University of Engineering & Technology, Qadirabad Cantonment, Natore 6431, Bangladesh*

Correspondence should be addressed to A. N. R. Reddy; amarnadha@gmail.com

Received 26 December 2016; Revised 23 February 2017; Accepted 7 March 2017; Published 12 April 2017

Academic Editor: Arghya Narayan Banerjee

Calcium based catalysts have been studied as promising heterogeneous catalysts for production of methyl esters via transesterification; however a few were explored on catalyst synthesis with high surface area, less particle size, and Ca leaching analysis. In this work, an active Razor shell CaO with crystalline size of 87.2 nm, S_{BET} of 92.63 m^2/g, pore diameters of 37.311 nm, and pore volume of 0.613 cc/g was synthesized by a green technique "calcination-hydro aeration-dehydration." Spectrographic techniques TGA/DTA, FTIR, SEM, XRD, BET&BJH, and PSA were employed for characterization and surface morphology of CaO. Two-step transesterification of *Jatropha curcas* oil was performed to evaluate CaO catalytic activity. A five-factor-five-level, two-block, half factorial, central composite design based response surface method was employed for experimental analysis and optimization of Jatropha methyl ester (JME) yield. The regression model adequacy ascertained thru coefficient of determination (R^2: 95.81%). A JME yield of 98.80% was noted at C (3.10 wt.%), M (54.24 mol./mol.%), T (127.87 min), H (51.31°C), and R (612 rpm). The amount of Ca leached to JME during 1st and 4th reuse cycles was 1.43 ppm ± 0.11 and 4.25 ppm ± 0.21, respectively. Higher leaching of Ca, 6.67 ppm ± 1.09, was found from the 5th reuse cycle due to higher dispersion of Ca^{2+}; consequently JME yield reduces to 76.40%. The JME fuel properties were studied according to biodiesel standards EN 14214 and comply to use as green biodiesel.

1. Introduction

The sustainability "strengthening the mechanisms for redistribution from the present to the future" has become a motto of all nations around the world, for promoting intrinsic scientific research methodologies into agriculture, materials, energy, economy, and even urban planning [1]. Despite multiphase research in energy, rising global warming and air pollution issues instigated by fossil fuel combustion besides limited petroleum fuel reserves have led to research for sustainable renewable energy sources. Fatty acid methyl ester (FAME), commercially known as biodiesels, introduced in the 1980s as a sustainable fuel energy resource for reducing greenhouse emissions [2]. FAME comprises monoalkyl ester of long fatty acids, typically produced by the transesterification of biologically produced feedstocks such as vegetable oil (VO), animal fats, and microalgae oils in the presence of methyl alcohol (MeOH) and a suitable catalyst [3, 4]. Transesterification reaction is a combination of three sequential catalyzed reactions (1)–(3) in which triglycerides (TG) of a VO were transformed to diglycerides (DG) and monoglyceride (MG) and finally as glycerol and methyl ester (ME) known as biodiesel [5]. *Jatropha curcas* Linnaeus, an euphorbia family member, has attained the researcher's attention as one of the best suited nonedible VO feedstock types due to its agromedical tangible interests as well as pro human food cycle nature, for biodiesel fuel (BF) production via transesterification [4]. Acid or base catalyzed transesterification of VO was largely reported in literature and also concluded on the use of heterogeneous catalysts for sustainable BF production [6, 7].

$$\mathrm{TG} + \mathrm{MeoH} \xleftrightarrow{\text{Catalyst}} \mathrm{DG} + \mathrm{ME} \quad (1)$$

$$\mathrm{DG} + \mathrm{MeoH} \xleftrightarrow{\text{Catalyst}} \mathrm{MG} + \mathrm{ME} \quad (2)$$

$$\text{MG} + \text{MeoH} \overset{\text{Catalyst}}{\longleftrightarrow} \text{Glycerol} + \text{ME} \quad (3)$$

Catalytic activity of a solid catalyst is highly influenced by its surface area and particle size distribution [8, 9]. Moreover, rate of a reaction among the reactants significantly accelerates with lower particle catalysts since it improves the diffusion forces over catalyst particle surfaces and better mass flow channels [8, 10]. In addition, this phenomenon ensures higher reaction rate through availability of large number of active reactant molecules that need a minimal activation energy. Calcium based catalysts demonstrate key promising characteristics that include higher basicity, lesser solubility, better reusability, low costs, and easy availability. A large number of studies have been devoted to investigate biodiesel applications of pure or mixed calcium catalysts [11–15]. Buasri et al. [10] produced biodiesel from palm oil using CaO catalyst which synthesized various seashells that include mussel, cockle, and scallop and reported surface areas (S_{BET}) of 89.91 m^2/g, 59.87 m^2/g, and 74.96 m^2/g, respectively. Shan et al. [16] studied Ca-based heterogeneous catalyst perspectives synthesized using rich waste materials such as bones, mollusk shells, egg shells, and industrial wastes besides catalytic activity and biodiesel applications of calcium catalysts prospects and challenges were discussed. Mohamed et al. [17] derived CaO from cockle shell by calcination at 850°C, while Nurdin [18] derived CaO catalyst from *Paphia undulata* shell wastes through calcination at 680°C for transesterification of *Jatropha curcas* oil (JCO) and Rubber oil to biodiesel. Choudhury et al. [11], Teo et al. [12], and Taufiq-Yap et al. [13] investigated the transesterification of JCO using CaO of S_{BET} 7.114 m^2/g; 9.2 ± 0.80 m^2/g; and 9.5 m^2/g and obtained a biodiesel of 89.36%, 90%, and 85%, respectively, while Margaretha et al. [19] experimented with *Pomacea* sp. shells produced CaO with pore volume of 0.04 cc/g and S_{BET} of 17 m^2/g for transesterification palm oil to biodiesel. Tan et al. [14] investigated the transesterification kinetics of waste cooking oil to biodiesel using CaO catalyst synthesized from ostrich and chicken-eggshells besides their S_{BET} of 71.0 m^2/g and 54.6 m^2/g, respectively. Islam et al. [20] synthesized nano-$CaCO_3$ with particle of 20 ± 5 nm diameter from cockle shells by grinding mechanically in the presence of dodecyl dimethyl betaine. De Sousa et al. [21] investigated transesterification kinetics of soybean oil using commercial CaO, egg shell CaO, carb shell CaO S_{BE} of 0.9 m^2/g, 4.3 m^2/g, and 4.0 m^2/g, and particle size of 56 nm, 184 nm, and 74 nm, respectively.

The significant transesterification reaction parameters that influence JME yield include catalyst loading, methanol to oil ratio, reaction time, heating temperature, and the stirring rpm [22–26]. Many researchers explored optimal parametric sufficiency over their minimum and maximum levels. The intrinsic impact of a parameter and their potential interactions to achieve the optimal FAME yield was investigated using the response surface methodology (RSM) as an optimization and statistical analysis tool [11, 22, 27]. RSM was widely adopted based on three designs of CCD; CCRD [22, 27]; and Box-Behnken design [11] for optimal FAME. Vicente et al. [28] testified over two factors, temperature (20°C–75°C) and catalyst concentration (0.2–1.8 wt.%), using sunflower oil in the presence of various homogeneous and heterogeneous catalysts. Goyal et al. [23] reported the impact of four reaction parameters including the methanol-oil ratio, reaction time, NaOH catalyst concentration, and temperature over transesterification of JCO. A CCD based four-factor-five-level was utilized to analyze the parametric impact on the FAME yield. An optimal FAME field of 98.3% was reported at 11 : 1 molar ratio, 1 wt.% catalyst, 54°C temperature, and 110 min of reaction time, while Dhingra et al. investigated Karanja [29] and Jatropha [30] biodiesels production optimization by considering five reaction parameters using the RSM coupled with GA [29]. Many studies reported that the choice of reaction parameters directly contributes in biodiesel conversion process and influences FAME yield. Also, it is noted that reaction parameters, both stirring speed and reaction time, were less studied.

The literature studies emphasize suitability of calcium catalyst for biodiesel production via transesterification. Besides, higher surface area, large pores, and lesser particle size of a catalyst enhance their catalytic efficacy of transesterification reaction [11–15]. *Ensis arcuatus* has been commonly found to be fishery food source in the sandy coastal locations of Pacific and Antarctic areas and regionally referred to as Razor clams. The study reports of Kanakaraju et al. [31], Akmar and Rahim [32], and Hossen et al. [33] demonstrate potential of Razor clams marine life and abundance in the state of Sarawak as well as in the west Malaysian provinces. The previous works on synthesis of calcium catalysts are very limited and have been focused on increasing catalyst surface area and lowering the particle size from naturally available renewable wastes such as aquatic seashells [18, 20, 21, 34–38]. However, according to the best of our broad literature survey, no work has reported on activated CaO nanocatalyst synthesis using Razor shells. Moreover, a very scant work was accounted on the study on kinetics of transesterification reaction parameters that include catalyst loading, methanol to oil ratio, heating temperature, stirring speed, and reaction time, which need to be undertaken.

In this study, CaO of high surface area and pores as well as lower particle size was synthesized from a seashell so as to result in an activated heterogeneous catalyst. Besides, the direct and interaction impacts of five reaction parameters on the FAME yield were proposed to be investigated over JCO two-step transesterification process. Activated CaO was synthesized using locally available seashell species, Razor shells. A laboratory scale experimental protocol "calcination-hydro aeration-dehydration" was developed for Razor shell CaO synthesis; besides, structural and morphological characteristics were analyzed. The transesterification reaction kinetics was studied by employing a CCD based on the five-factor-five-level, two-block, half factorial, RSM model. JME production optimization protocol using active Razor shell CaO catalyst is shown in "Scheme 1." The catalyst stability, reusability, and leaching were investigated. The synthesized JME fuel properties were tested according to the biodiesel standards EN14214.

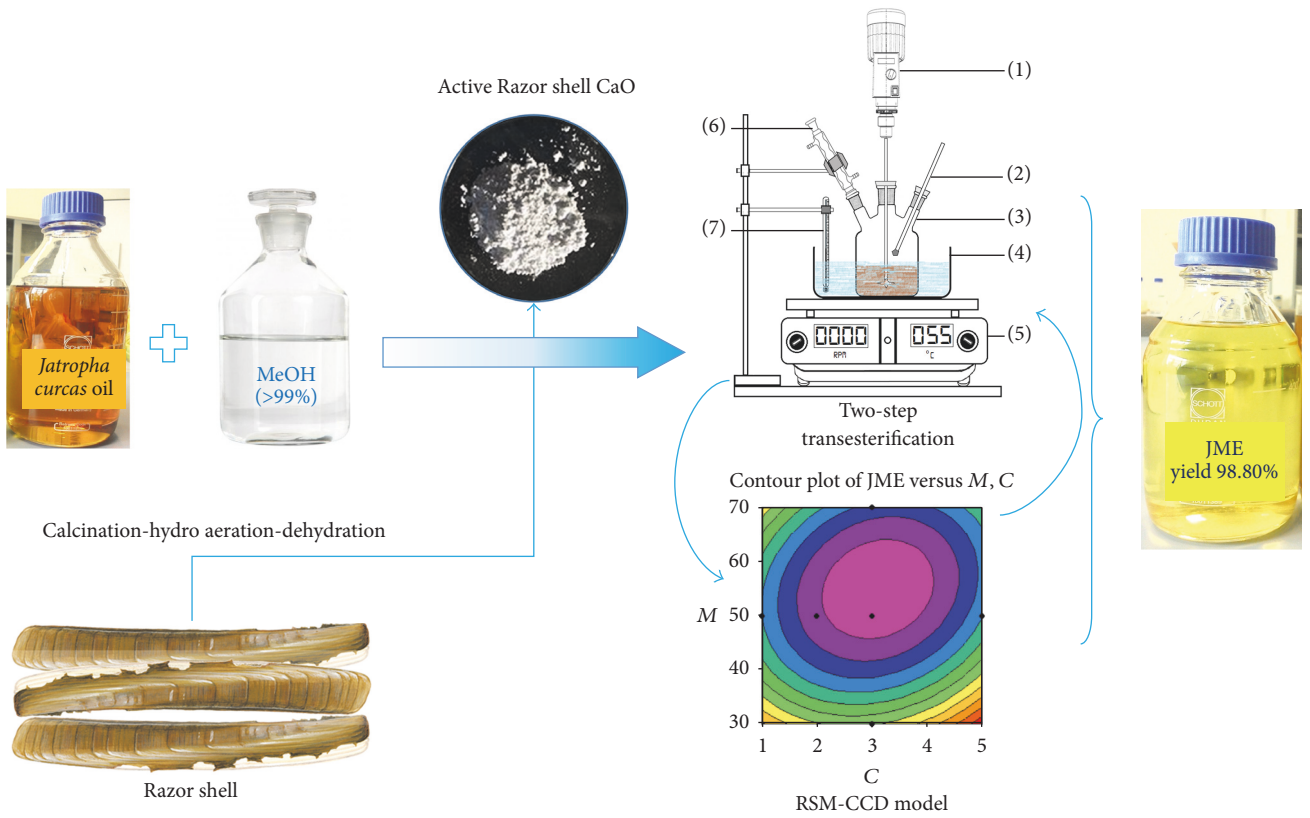

Scheme 1: Jatropha methyl ester production optimization using active Razor shell CaO catalyst.

2. Material and Method

The *Jatropha curcas* seeds were obtained from a Jatropha farm, Wahaba Sdn. Bhd., situated in Sarawak, Malaysia. *Jatropha curcas* oil (JCO) was extracted mechanically using an oil expelling machine from their dried seeds. The crude JCO was used as extracted without any processing like purification or refining. JCO fatty acid profile was determined by the gas chromatography and the results are as indicated in Table 6. The acid value (A) and saponification value (S) of JCO were measured as 29.46 mg KOH/g and 210.04 mg KOH/g, respectively, by utilizing a standard procedure [39]. The molecular weight (M) of JCO was resulted as 932 g/mol. by the equation $M = (56.1\times1000\times3)/(SV-AV)$ [39]. Laboratory grade chemicals that include sulfuric acid (99.9%), methyl alcohol (>99%), potassium hydroxide (95%), calcium oxide (CAS.NO.0001305788), and double distilled deionized water were utilized. All experiments were conducted at the Energy Laboratory, Department of Mechanical and Manufacturing Engineering, Faculty of Engineering, Universiti Malaysia Sarawak (UNIMAS), Malaysia.

2.1. Preparation of Active Razor Shells CaO Catalyst. Razor shells were collected from a local community market at Muara Tebas, Sawarak, Malaysia. The CaO catalyst was synthesized following "calcination-hydro aeration-dehydration" of the Razor shell. The synthesis protocol is adopted as described before by Niju et al. [40, 41] and modified to get a fine Razor shell powder. In a nutshell, about 500 gm of Razor shells was thoroughly water washed and dried overnight at 105°C in a hot air oven (IMPACT, Scotland, UK) [42]. The dried Razor shell was finely crushed using a heavy duty professional blender (OmniBlend V, imbaco, Australia) and then sieved using an 80 μm mesh. The micron-sized Razor shells powder was calcinated in a high temperature muffle furnace (KSL-1700X-A4, MTI Corporation, USA), at a target temperature of 850°C for 2.5 h. At a calcine temperature of 850°C, $CaCO_3$ of Razor shell decomposes as CaO and CO_2. The fine CaO powder was refluxed in water for 6 h at 60°C. Simultaneously, the mixture was aerated using spherical and cylindrical air stone bubbler setup fitted with a Hi-blow air pump (HAP-60, 0.01 Mpa, 60 w Hailea) and then the mixture was allowed to settle for 2 h. Continuous aeration oxygenates refluxing mixture and precipitates heavy dirt and solid particles which results in refined highly pores Razor shell CaO particles. The catalyst was filtered and dried overnight at 120°C in an oven [42]. The refined Razor shell solid powder was grounded for high grade fine catalyst particles utilizing a Planetary Ball mill (PM 400, Retsch, Germany) at 250 rpm for 2 h. Calcination of fine Razor shell CaO was carried out for 3 h at 600°C so as to transform hydroxides to oxide form through dehydration. Accordingly, an active Razor shell CaO catalyst was synthesized following "calcination-hydro aeration-dehydration" protocol.

2.2. Characterization of Razor Shells CaO Catalyst. To investigate the organic structural features of Razor shell CaO catalyst, newly synthesized CaO and lab grade CaO samples were

characterized using infrared spectrometer (Perkin Elmer, 100 series) over wavelengths 4000 to 280 cm^{-1}. Thermogravimetric analyzer equipped with high temperature furnace (Mettler-Toledo, Switzerland) was employed for thermogravimetric and differential thermal analysis (TG/DTA) of Razor shell catalyst. Thermal analysis of samples was performed 35°C–1000°C at a heating rate of 10°C/min and airflow of 100 ml/min. Razor shell CaO catalyst and lab grade CaO crystalline features were studied employing X-ray diffraction (XRD) method (Shimadzu 6000) over 20–80°C at a scanning angle of 2θ and frequency of 2°C per minute. Scherrer's equation, $D = 0.9\lambda/\beta\cos\theta$, was applied to calculate CaO particle average crystalline size, where "D" denotes average crystalline size of CaO in nm, λ equals 1.542 Å, X-ray radiation wavelength, "β" denotes full width at half maximum intensity in radians, and "θ" denotes Bragg angle in degrees. Razor shell CaO catalyst surface morphology was analyzed with scanning electron microscopy (SEM TM3030, Hitachi, Japan). The newly synthesized Razor shell CaO catalyst surface area, pore diameter and pore volume, calcined nonaerated CaO, unclacined Razor shell, and reference-CaO powder samples were investigated utilizing the BET (Brunauer-Emmett-Teller) and BJH (Barrett-Joyner-Halenda) protocols (Autosorb iQ-AG-C, Quantachrome instruments, USA). Both aerated and nonaerated CaO samples of Razor shell's particle size distribution were studied using particle size distribution analyzer (PSA 1090, 0.04 μm–500 μm, CILAS, France). The basic strength (H_) of Razor shell catalyst was determined by employing Hammett indicators. Typically, a solution mixture of 1 ml of Hammett indicator and 20 ml of methanol was prepared and added to 25 mg of catalyst sample. The contents were shaken well to attain homogeneity and left for 2 h to equilibrate and then catalyst color change was noted [43]. The following Hammett indicators were utilized: phenolphthalein (H_ = 8.2), thymolphthalein (H_ = 10.0), 2,4-dinitroaniline (H_ = 15.0), and 4-nitroaniline (H_ = 18.4). By adding a Hammett indicator to the catalyst sample, if it displays a change in color which infers that basicity of the catalyst is stronger compared to the Hammett indicator used, on the contrary the catalyst sample is to be labeled as a weaker than the probe Hammett indicator [44].

2.3. Jatropha Methyl Ester Production. Jatropha methyl ester (JME) production was carried out by following an in-house laboratory protocol. The high free fatty acids (FFA) and moisture contents of JCO strongly influence JME production through the catalyzed transesterification reaction [45]. JCO of FFA value > 3% and moisture content > 1 wt.% which lead to saponification and oil hydrolysis besides reducing rate of biodiesel yield [46]. Hence, a two-step transesterification process was adopted [47]. The first step is acid esterification in which FFA of JCO reduced to a suitable minimum level followed by the second step which is base catalyzed transesterification [48]. The successive steps which involved acid esterification and catalyzed transesterification are explained in the following sections.

2.4. Acid Esterification. A digital hot plate magnetic stirrer mixer (MS300-BANTE make 300°C, 2 L, 220 V, 1250 rpm) and a 500 ml two-neck flat bottom glass reactor are attached to a water cooled reflex condenser used for the acid esterification of JCO. In order to improve the JCO conversion process and enhance the JME yield, esterification was carried out using methanol and concentrated H_2SO_4 as a catalyst as mentioned in (4). An amount of 100 ml JCO was preheated at 110°C for 30 min to get moisture-free oil. A mixture of 60% (v/v) methanol and 1% (v/v) catalyst to JCO was prepared and added to the JCO. The mixture was vigorously stirred at 200 rpm and then heated to 50°C for 1 h. After the reaction, the reactant mixture was allowed to settle for 1 h and then washed successively thrice using double distilled deionized water. Finally, the oil portion was duly dried at 110°C to prepare moisture-free oil. As a result of acid esterification, FFA of JCO was noted all in a minimum of 1% with an esterification rate of 98.4%. Thus, the esterified JCO was suitable for the transesterification with base catalyst [48].

$$\mathrm{RCOOH} + \mathrm{CH_3OH} \xrightleftharpoons{\mathrm{H_2SO_4}} \mathrm{RCOOCH_3} + \mathrm{H_2O} \quad (4)$$

2.5. Transesterification of Esterified JCO. The transesterification of the esterified JCO with newly synthesized Razor shell CaO catalyst was carried out in a 500 ml three-neck flat bottom glass reactor fitted together with an overhead stirrer (IKA RW 20 Digital Dual-Range Mixer, speed 60 to 500/240 to 2000 rpm), a sampling port, and a water cooled reflex condenser. A digital hot plate was employed for providing a variable heat input as desired for the transesterification reaction process. The reactor experimental setup was immersed in a water bath to keep the uniform temperature levels throughout the reaction process. The schematic of the experimental setup is shown in Figure 1. A mix of methanol of 30 to 70 mol./mol.% and Razor shell CaO catalyst of 1 wt.% to 5 wt.% was thoroughly mixed for one hour and then transferred to the glass reactor for each batch of experiments. The transesterification reaction was performed over discrete operating parameters that include heating temperature of 40°C to 60°C, stirring speed of 500 rpm to 700 rpm, and a reaction time of 60 min to 180 min. These parametric ranges were ascertained with published literature [22–24, 49].

2.6. Design of Experiments for Optimal JME Yield. The flow of the JME yield optimization was broadly executed in four sequential operations starting with the review, experimental design, modeling and optimization, and results validation. The intrinsic actions followed in each operation stage together with decision flow are shown in Figure 2. In this study, five significant independent transesterification reaction parameters which influenced the JME yield include Razor shell CaO catalyst loading (C), methanol to oil ratio (M), reaction time (T), heating temperature (H), and the stirring rpm (R) which have been considered for the optimization of % JME yield. The effects of five significant reaction parameters together with intrinsic interactions were devised by utilizing a central composite design (CCD) based on the half-fraction model response surface statistical model. The transesterification experimental data obtained were then fit to a full quadratic equation as specified in (5) to analyze the

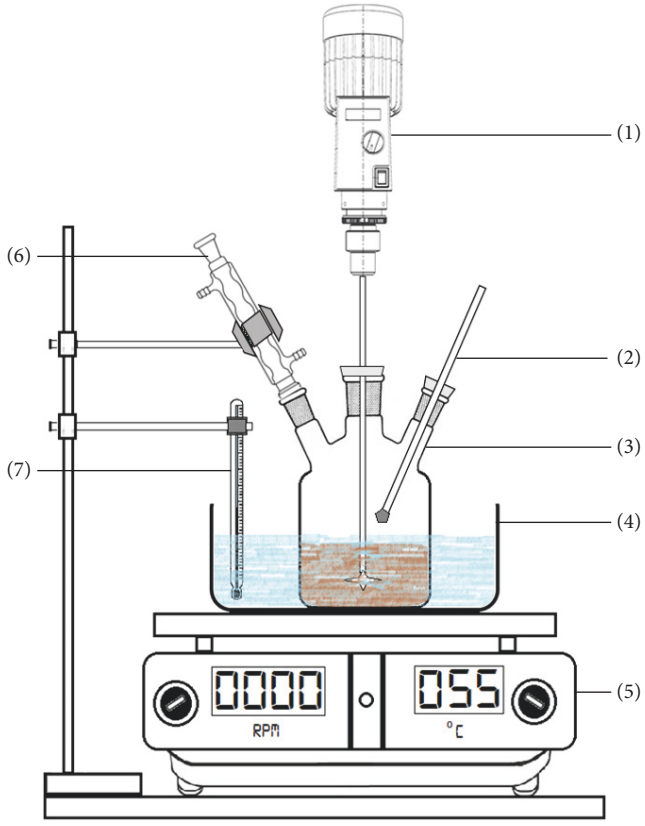

(1) Digital overhead stirrer
(2) Sampling port
(3) Three-neck glass reactor
(4) Water bath tub
(5) Digital hot plate
(6) Reflex condenser
(7) Thermometer

Figure 1: Transesterification experimental setup for JME production.

response variable, % JME yield, through the response surface regression procedure.

$$Y = \beta_0 + \sum_{i=1}^{n} \beta_i k_i + \sum_{i=1}^{n} \beta_{ii} k_i^2 + \sum \sum_{i<j=1}^{n} \beta_{ij} k_i k_j + \varepsilon. \quad (5)$$

The symbolic notations of (5) are as follows: "Y" is the predicted response for % JME yield; "β_0" is the constant coefficient; "β_i, β_{ii} and β_{ij}" are the regression coefficients of intercept, linear, quadratic interactions; k_i and k_j are the coded independent process parameters; and "ε" is the residual of the predicted and experimental value, known as standard error. The five significant parameters were set independently within the following ranges: $1 \leq C$ (wt.%) ≤ 5, $30 \leq M$ (mol./mol.%) ≤ 70, $60 \leq T$ (min) ≤ 180, $40 \leq H$ (°C) ≤ 60, and $500 \leq R$ (rpm) ≤ 700. Considering each factor at five levels, 33 base experimental reaction iterations were concluded from a CCD of two-block, half-fraction model, which corresponds to sixteen cubic points, six center points in the cube, ten axial points, and one center point at the axial level. For a CCD the numerical value of alpha, $\alpha \pm 2$, is a measure of the distance that keeps each of the axial design points from the center in evolution of the factorial levels [27]. In Table 1, the actual levels of individual parameters were tabulated representing their coded and uncoded values. The redundancy in datasets and results was minimized by performing all the experiments in a random run order. The Minitab® 16.2.1 software was employed for performing the analysis of variance (ANOVA) of the model together with CCD based response surfaces generation and % JME yield optimization. A Minitab 16.2.1 software was utilized for the response surface regression analysis and ANOVA of the designed model. The regression model was presented in (5) and validation was ensured through the confirmatory experiments, besides analysis of corresponding contour and surface plots.

2.7. Study of Razor Shell CaO Reusability, Leaching Analysis, and Transesterification with Reference Catalyst. The Razor shell CaO catalyst was recovered by centrifuging the transesterification reactant samples at 4000 rpm for 60 min. The precipitated CaO was then washed in four sequential repeats with *n*-hexane to remove Jatropha oil residues and then dried overnight in a forced air convection oven followed by recalcination at 850°C for 2 h before reuse. The oil portion separated was washed using double distilled deionized hot water successively for four times to clear away the traces of methanol and catalyst from the samples followed by drying over 110°C in order to obtain a pure JME. Furthermore, all the experiments were conducted using the variant operating parameters to investigate their specific impact on the JME yield. The biodiesel obtained from each reusability cycle was tested using an atomic absorption spectrometer-AAS (AA-7000, Shimadzu, calcium "422.7 nm" hollow cathode lamps as radiation source) and to measure the amount of calcium ions (Ca^{2+}) concentration that leached into the JME samples. The newly synthesized Razor shell CaO catalytic activity was evaluated in comparison with a lab grade CaO (CAS.NO.0001305788). Before being used, the lab grade CaO catalyst was dehydrated at 105°C for 2 h in a hot air oven. Further, the reused Razor shell CaO catalyst surface morphology was analyzed using SEM (TM3030, Hitachi, Japan). Five successive cycles of relative transesterification were carried out using esterified JCO under similar experimental conditions and standard ratios.

2.8. Jatropha Methyl Ester Fuel Properties Analysis. The specific JME fuel properties that include density at 15°C, calorific value, flash point, cetane value, specific gravity at 15°C, viscosity at 40°C, water content, ash content, acid value, monoglyceride, diglyceride, triglyceride, free glycerine, total ester content, and total glycerine contents were evaluated with a fuel property testing equipment built on the ASTM standards (D2624, D3828) and European standards (EN 14105) such as calorimeter, fuel test kit, and gas chromatograph (Shimadzu-GC-2010 Plus) fitted with a flame ionization detector FID-2010 Plus and a capillary column of size 30 m × 0.25 mm × 0.25 μm.

3. Results and Discussion

3.1. Analysis of Razor Shell CaO Characteristics. Thermogravimetric analysis (TGA) and differential thermal analysis

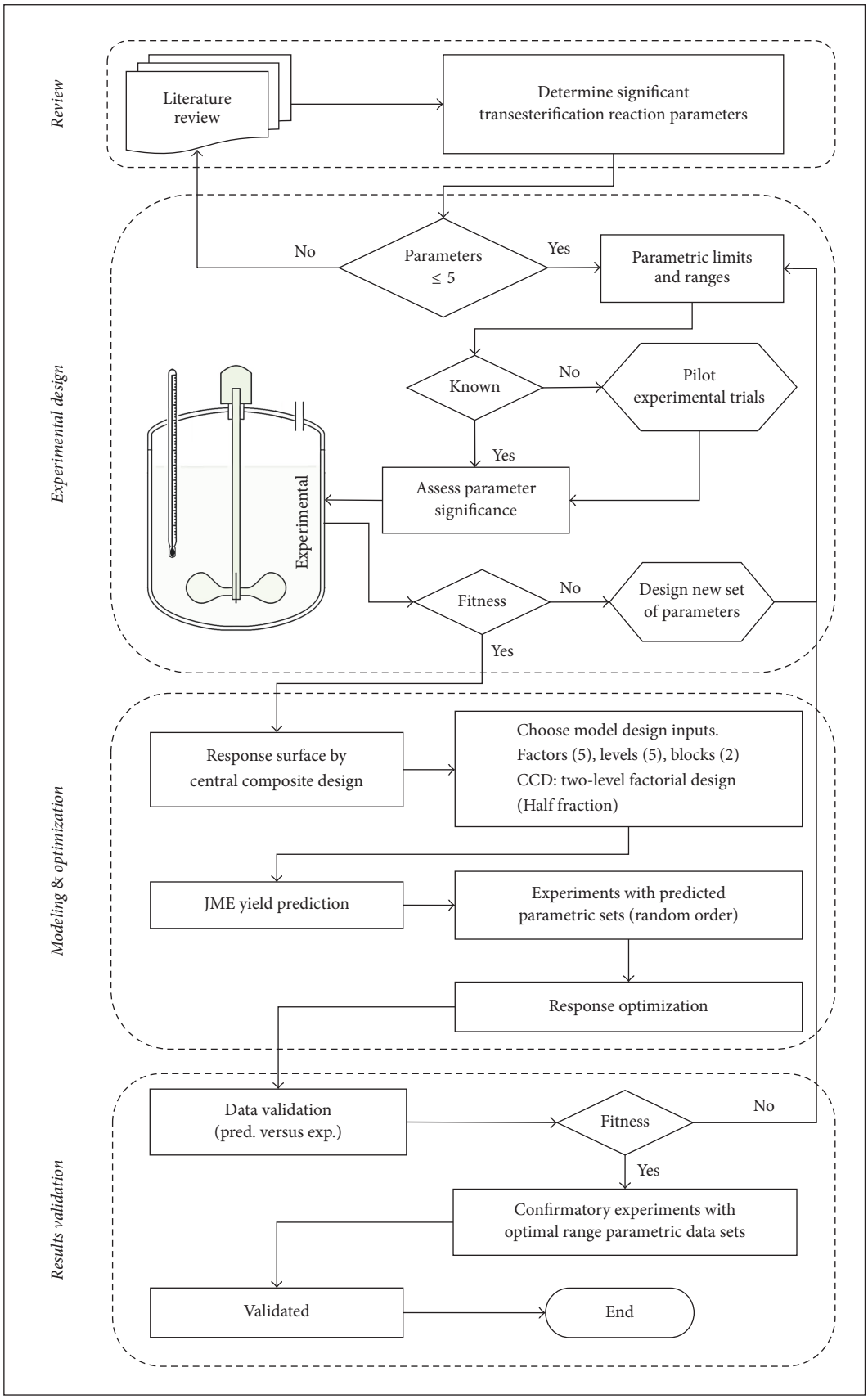

Figure 2: Schematic of optimal JME yield using experimental, modeling, and optimization protocol (customized based on [22]).

Table 1: Factors and their uncoded levels.

Uncoded variable	Symbol	Levels				
		−2	−1	0	1	2
Razor shell CaO catalyst loading (wt.%)	C	1	2	3	4	5
Methanol to oil ratio (mol./mol.%)	M	30	40	50	60	70
Reaction time (min)	T	60	90	120	150	180
Heating temperature (°C)	H	40	45	50	55	60
Stirring speed (rpm)	R	500	550	600	650	700

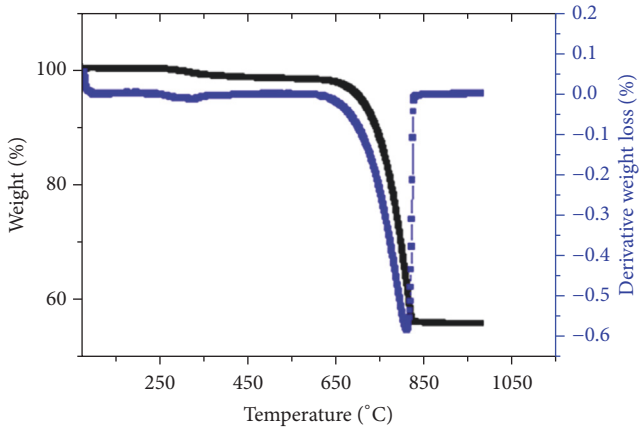

Figure 3: Thermal analysis (TGA/DTA) of Razor shells.

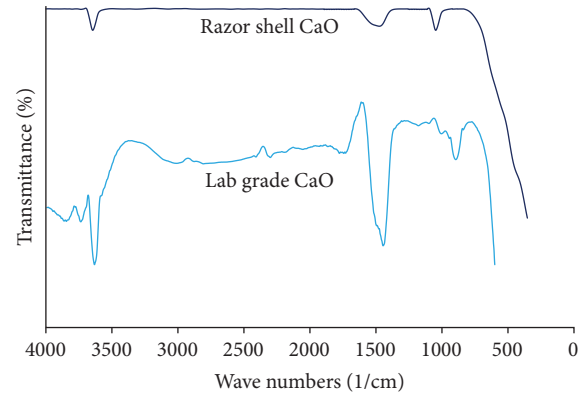

Figure 4: IR spectra of calcined lab grade CaO and Razor shell CaO.

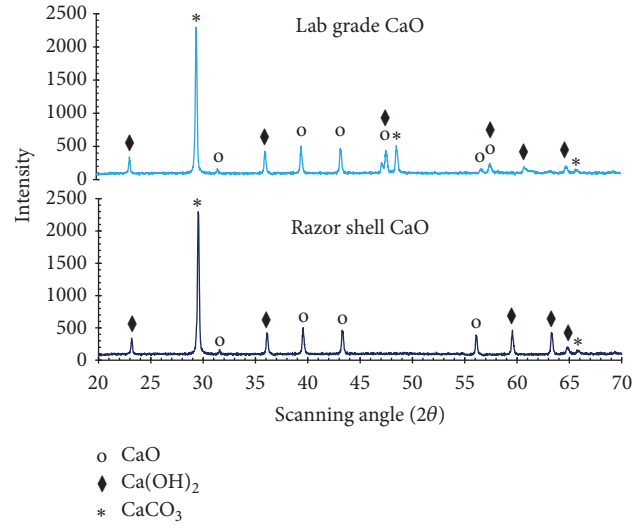

Figure 5: XRD spectral graph of analysis of calcined lab grade CaO and Razor shell CaO.

(DTA) of uncalcined Razor shell were shown in Figure 3. The weight loss indicates quantitative composition of Razor shell catalyst. Also, the exothermic and endothermic measurements presented using DTA curve which shows thermal influence on oxidation degradation and physiochemical changes. From Figure 3 till 650°C, TGA curve continued constant and then decomposition initiated over 850°C. A sharp TGA slope between 650°C and 850°C is observed which conforms $CaCO_3$ thermal decomposition. Further, DTA curve is consistent with TGA and at a temperature of 820°C, DTA indicates $CaCO_3$ endothermic conversion to a constant CaO. Therefore, the TGA/DTA analysis confirms calcination of Razor shells over temperature range of 850°C to convert $CaCO_3$ to CaO. This result is in agreement with Tan et al. [14] and Roschat et al. [50].

The infrared spectra of Razor shell synthesized CaO and lab grade CaO powder samples are shown in Figure 4. The absorption bands over wavelength < 700 cm^{-1} were strong besides broad medium absorption bands at 990 cm^{-1}, 1430 cm^{-1}, and 3640 cm^{-1} which attributes presence of Ca-O stretching. According to the reports of Tan et al. [14], McDevitt and Baun [51], Nasrazadani and Eureste [52], and Zaki et al. [53], the strong IR spectral absorption over wavelengths 400 cm^{-1} and 290 cm^{-1} signifies Ca-O which confirms CaO presence. Further, weak absorption wavelengths > 3700 cm^{-1} specifically 3722 cm^{-1} and 3807 cm^{-1} were present due to carbonyl "C=O" and hydroxyl "O-H" groups asymmetric bending. As reported by De Sousa et al. [21], Tan et al. [14], and Margaretha et al. [19], the hygroscopic nature of catalyst is highly prone to absorb carbon dioxide and moisture from the atmosphere and subsequently forms $CaCO_3$ and $Ca(OH)_2$.

The crystalline structural information of Razor shell synthesized CaO and lab grade CaO obtained from XRD analysis is shown in Figure 5. The Razor shell synthesized CaO XRD spectral graph shows clear diffraction peaks at scanning angles (2θ) of 23.18°, 29.54°, 36.14°, 39.56°, 43.28°, 56.16°, 59.54°, and 63.34°, whereas lab grade CaO shows peaks at 23.18°, 29.54°, 36.14°, 39.56°, 43.28°, 47.2°, 47.68°, 48.68°, 56.16°, 56.94°, 57.58°, 59.54°, 61.08°, and

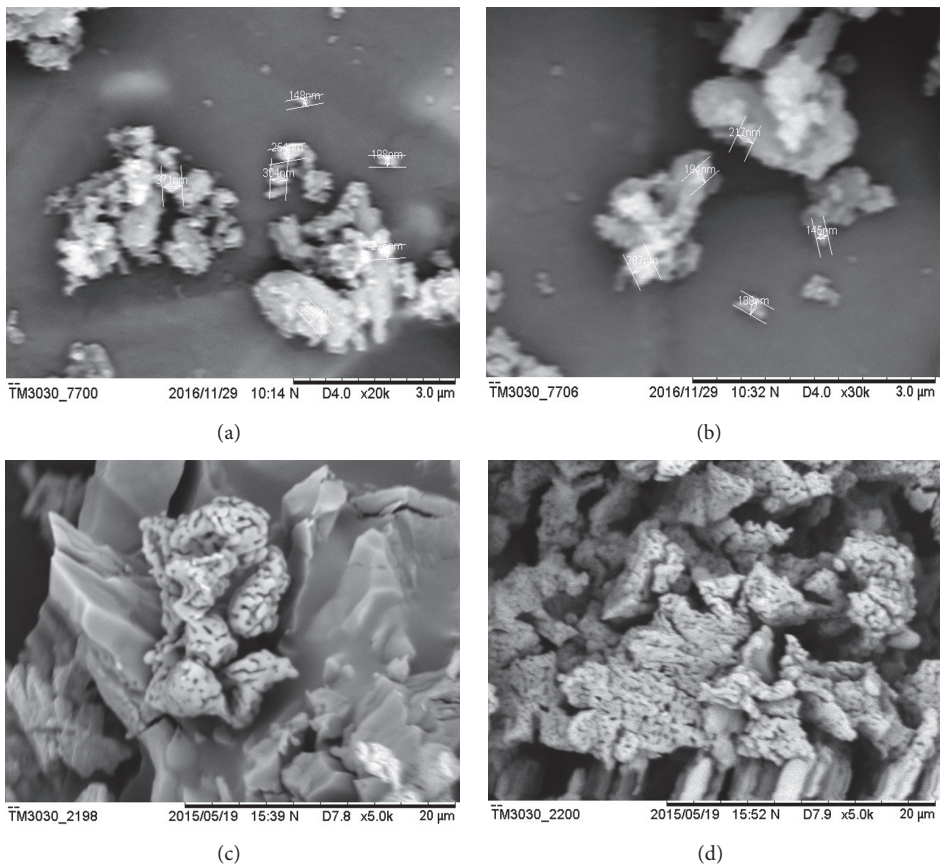

Figure 6: SEM monograms of (a, b) hydro aerated calcined Razor shell CaO; (c, d) calcined lab grade CaO.

63.34°. The diffraction patterns were verified and consistent according to JCPDS file number 00-037-1497 as well with published reports by Mirghiasi et al. [54], Teo et al. [55], Chen et al. [56], De Sousa et al. [21], and Tan et al. [14]. The "calcination-hydro aeration-dehydration" resulted in removal hydroxyl and carbonyl phases and causes of a pure CaO. However after thermal decomposition high hygroscopic nature of calcium and minor moisture absorption at lab temperature cause formation of a few $Ca(OH)_2$. According to Scherrer's equation calculations the average crystalline sixe of Razor shell CaO is noted as 87.2 nm.

The SEM surface morphology of hydro aerated and calcined Razor shell CaO was measured at a microscopic magnification of 20000x and 30000x with 0.3 μm, shown in Figures 6(a) and 6(b). The SEM monograms of calcined lab grade CaO surface morphology were viewed at a magnification of 5000x shown in Figures 6(c) and 6(d). The Razor shell CaO SEM monograms encompass a number of particles in regular sizes of 145 nm–371 nm together with agglomerates observed. This can be attributed to structural changes of isolated isotropic calcium oxide particles after hydro aeration followed by calcined at high temperatures while $CaCO_3$ constituents decompose into CaO and CO_2, as a result of decreases in particle sizes. These results are fully in accordance with investigation reports of Tan et al. [14] and Buasri et al. [10].

The BET and BJH analysis of Razor shell synthesized, hydro aerated, and nonaerated calcined CaO and uncalcined Razor shell together with reference catalyst samples had determined S_{BET} of 92.63 m^2/g, 85.27 m^2/g, 5.21 m^2/g, and 36.6 m^2/g; pore diameters of 37.311 nm, 33.342 nm, 11.355 nm, and 13.861 nm; and also total pore volume of 0.613 cc/g, 0.423 cc/g, 0.0121 cc/g, and 0.126 cc/g, respectively. Compared to literature reports, Tan et al. [14] derived calcium catalyst from chicken-eggshells (54.6 m^2/g) and ostrich-eggshells (71.0 m^2/g); Buasri et al. [10] synthesized mussel shells (89.91 m^2/g), cockle shells (59.87 m^2/g), and scallop shells (74.96 m^2/g), while Margaretha et al. [19] reported CaO of 17 m^2/g. The S_{BET} of Razor shell CaO is relatively high; moreover, the resulted pore diameter ranges within mesopores (2 nm–50 nm) demonstrate high value of the catalyst surface area together with their suitability for adsorption, catalytic, and energy storage applications [57]. Hence, the CaO of Razor shells synthesized through "calcination-hydro aeration-dehydration" is an active catalyst owing to high pores and external surface area. Further, the Razor shell synthesized CaO particles demonstrated bimodal particle sizes (Figure 7). The particle sizes of hydro aerated calcined Razor shell CaO are in the range of 0.82 μm–5.55 μm with a mean particle size of 2.97 μm; meanwhile the nonaerated calcined Razor shell CaO showed particle sizes over 0.8 μm–9.25 μm and mean size of 4.37 μm. The difference

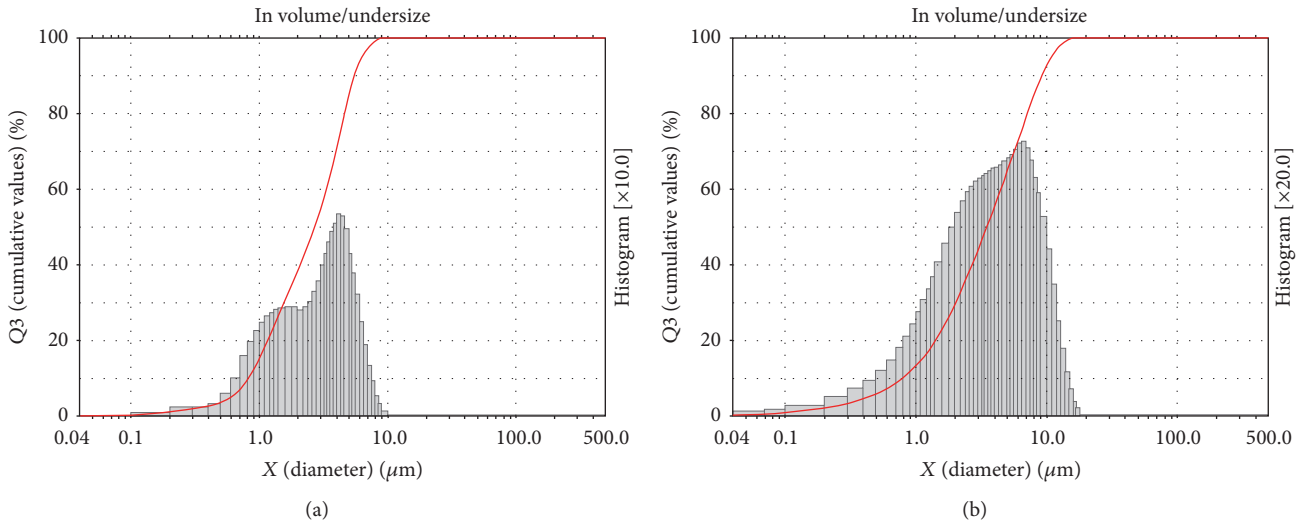

Figure 7: Particle size distribution grid of (a) hydro aerated calcined Razor shell CaO; (b) nonaerated calcined Razor shell CaO.

in mean and median particle sizes of hydro aerated and nonaerated calcined Razor shell CaO is significant. Therefore the "calcination-hydro aeration-dehydration" caused a mix of micro- and nanocatalyst particles together with few large agglomerates. The results are comparable and consistent with the literature reports of Tan et al. [14] and Kesić et al. [58]. By adding Hammett indicators to Razor shell synthesized CaO, the catalyst samples successfully changed the color of phenolphthalein (H_ = 8.2) from being colorless to pink, thymolphthalein (H_ = 10.0) from being colorless to blue, and 2,4-dinitroaniline (H_ = 15.0) from yellow to mauve, respectively. Conversely, the catalyst was unsuccessful to change the color of 4-nitroaniline (H_ = 18.4). Hence, the newly synthesized CaO catalyst basic strength was labeled as $15 < H_ < 18.4$ and therefore the basic strength of newly synthesized CaO catalyst was a strong basicity for JCO. The basicity of Razor shell CaO agreed with the published results for CaO, synthesized from waste materials [15, 43, 44]. The Razor shell CaO catalyst was synthesized following "calcination-hydro aeration-dehydration" protocol which resulted in smaller particle size as well as greater surface area. According to Thiele [59], Buasri et al. [10], and Teo et al. [8] catalyst of higher surface area and lesser particle size improves its catalytic activity and reaction kinetics rapidly by refining the particle diffusion drawbacks. Henceforth the Razor shell CaO is labeled as "an active catalyst."

3.2. Jatropha Methyl Ester Production Analysis. The JME was produced by transesterification of esterified JCO using methanol and Razor shell CaO catalyst and, in addition, three controlled parameters such as reaction time, heating temperature, and stirring rpm. The minimum FFA condition from the acid esterification was opted for Razor shell CaO catalyzed transesterification of Jatropha triglycerides. The standard protocol comprising experimental, modeling and optimization, and validation operation processes as presented in Figure 2 was followed in order. The selection of optimal experimental parametric values was determined on the basis of their relative impact evaluations while optimizing the JME yield, which is discussed in the following sections.

3.3. Regression Model Analysis. The experimental results of second step pf transesterification reaction were analyzed using a two-block, half-fraction CCD statistical model as tabulated in Table 2. The estimated response surface regression coefficients for optimal JME using the uncoded units are as listed in Table 3. A regression modal equation that was fitting the JME yield as a response parameter to the other five significant reaction parameters in terms of their uncoded values is as given in

$$\begin{aligned} Y = {} & 100.071 + 0.262C + 6.707M + 4.002T + 4.515H \\ & + 0.931R - 11.439C^2 - 14.186M^2 - 14.224T^2 \\ & - 11.824H^2 - 6.524R^2 + 4.379CM + 0.493CT \\ & - 0.846CH - 0.193CR - 2.021MT - 4.479MH \\ & + 0.721MR - 1.393TH + 3.754TR - 1.707HR. \end{aligned} \quad (6)$$

The sign of regression coefficient is an indication of the effect of the corresponding term being synergetic or antagonistic, on the response parameter. Referring to the mathematical equation (6) all the five parameters in their linear form show a positive effect, whereas the quadratic terms of these parameters have a negative effect on the JME yield. However, the ten interaction terms have a mix of both positive and negative effects on the JME yield, which will be discussed in the later part of this section, in detail.

The regression modal analysis of variance (ANOVA) was utilized to study the adequacy of the model [60]. Table 4 summarizes the ANOVA for the model designed. The value of the coefficient of determination R^2 for the model was noted as 95.81%, which implies the fitness of the regression model in attributing good correlation between the percentage of JME yield and five transesterification parameters studied [61],

Table 2: The CCD design matrix for JME yield prediction (randomized).

Type of points and runs	Run	Block	Coded parameters					JME yield	
			C	M	T	H	R	Predict.	Exp.
Cubic points $\alpha = \pm 1$ (16 runs)	1	1	1	−1	−1	−1	−1	74.81	74.40
	2	1	1	1	1	1	1	73.52	72.40
	3	1	1	−1	1	−1	1	82.58	83.40
	4	1	1	−1	−1	1	1	85.47	85.60
	5	1	1	−1	1	1	−1	78.76	77.80
	6	1	1	1	1	−1	−1	80.80	79.60
	7	1	1	1	−1	1	−1	88.26	89.00
	8	1	−1	1	1	1	−1	87.36	86.40
	9	1	1	1	−1	−1	1	83.90	83.20
	10	1	−1	-1	−1	1	−1	79.14	78.20
	11	1	−1	1	−1	1	1	87.21	89.20
	12	1	−1	−1	−1	−1	1	88.71	89.00
	13	1	−1	1	−1	−1	−1	87.78	87.00
	14	1	−1	−1	1	−1	−1	84.08	82.60
	15	1	−1	−1	1	1	1	90.09	91.00
	16	1	−1	1	1	−1	1	91.59	91.80
Axial points $\alpha = \pm 2$ (10 runs)	17	2	−2	0	0	0	0	90.19	87.20
	18	2	2	0	0	0	0	90.71	93.40
	19	2	0	0	0	−2	0	81.00	84.00
	20	2	0	0	−2	0	0	94.41	93.00
	21	2	0	−2	0	0	0	83.66	83.20
	22	2	0	0	0	0	2	91.67	93.00
	23	2	0	2	0	0	0	85.55	86.60
	24	2	0	0	0	0	−2	94.58	94.40
	25	2	0	0	2	0	0	94.44	95.60
	26	2	0	0	0	2	0	96.30	96.00
Center points in cube $\alpha = 0$ (6 runs)	27	1	0	0	0	0	0	98.25	98.00
	28	1	0	0	0	0	0	98.25	98.00
	29	1	0	0	0	0	0	95.26	97.60
	30	1	0	0	0	0	0	95.26	97.60
	31	1	0	0	0	0	0	98.25	98.00
	32	1	0	0	0	0	0	98.25	97.80
Center points in axial (1 run)	33	2	0	0	0	0	0	99.89	98.00

and also to confess the successful integrity of the regression equation among the experimental data, appropriately. The difference between the coefficients of determination (R^2) and the correlation ($R^2_{\text{adj}} = 87.81\%$) at large discloses the presence of the nonsignificant parametric terms in the designed regression model. The comparative graph of Figure 9 shows coherence between JME predicted and experimental yields. Besides, the f-test and P values were the indications of modal and each regression coefficient significance, respectively [30].

3.4. Transesterification Reaction Parameter Effects Analysis on JME Yield. Each of the five transesterification parameters' significance and their effect on JME yield were tested and analyzed in terms of their parametric interactions through the regression model (6) as well as the ANOVA. From the data reported in Table 4, the linear form of the parametric terms of methanol to oil ratio (M), reaction time (T), and heating temperature (H) was having relatively higher impact on the JME yield owing to the high F-values as compared to the other parameters catalyst loading (C) and stirring rpm (R). The interaction between any two selected parameters on % JME yield was analyzed by holding the remaining three reaction parameters at their median levels.

3.4.1. Catalyst Loading (C). Catalyst loading is one of the key parameters that influence the production of JME in terms of both JME yield percentage and its quality [62–64]. The effect of the Razor shell CaO catalyst loading interactions with other reaction parameters of the reaction time, methanol to oil ratio, heating temperature, and stirring speed was plotted, respectively, in the contour plots shown in Figures 8(a), 8(b), 8(c), and 8(d). Though the catalyst loading was carried through 1 wt.%–5 wt.%, JME yield was significant, ">98%" over 2 wt.%–4 wt.%. From the regression equation

Table 3: Estimated response surface regression coefficients for optimal JME yield using uncoded units.

Term	Coef.	SE coef.	T	P
Constant	100.071	1.0485	95.447	0.000
Block	−1.819	0.4824	−3.771	0.003
Linear				
C	0.262	1.0603	0.247	0.810
M	6.707	1.1903	5.635	0.000
T	4.002	1.0721	3.733	0.003
H	4.515	1.0907	4.140	0.002
R	0.931	1.0721	0.868	0.404
Quadratic				
C^2	−11.439	1.9574	−5.844	0.000
M^2	−14.186	1.9517	−7.269	0.000
T^2	−14.224	1.9047	−7.468	0.000
H^2	−11.824	1.9047	−6.208	0.000
R^2	−6.524	1.9047	−3.425	0.006
Interaction				
$C \times M$	4.379	3.0693	1.427	0.181
$C \times T$	0.493	2.6488	0.186	0.856
$C \times H$	−0.846	2.7161	−0.312	0.761
$C \times R$	−0.193	2.6488	−0.073	0.943
$M \times T$	−2.021	3.0062	−0.672	0.515
$M \times H$	−4.479	3.0693	−1.459	0.172
$M \times R$	0.721	3.0062	0.240	0.815
$T \times H$	−1.393	2.6488	−0.526	0.609
$T \times R$	3.754	2.7161	1.382	0.194
$H \times R$	−1.707	2.6488	-0.645	0.532

(6), it is evident that the catalyst loading has a positive impact on the JME yield; that is, JME yield was proportional to the utilization of 1 wt.%–4 wt.% catalyst. It was noted that the lower catalyst loading (<2 wt.%) does not result in a productive JME yield. Furthermore, the higher catalyst loading (>4 wt.%) leads to the catalyst secondary reactions with other reactants which result in the reduction of JME yield [65]. The calcium based catalysts have demonstrated leaching tendency to the biodiesels during transesterification [12, 46, 47]. According to the biodiesel standards, EN 14214:2008, allowable concentration of group-I (Na + K) and group-II (Ca + Mg) is max. 5.0 mg/kg in the biodiesel samples while the residues of excess metal oxides act as impurities in the biodiesel fuel produced [66]. The catalyst loading interactions with methanol to the oil ratio ($C \times M$) and transesterification reaction time ($C \times T$) resulted in positive interactions. In contrast, interactions with reactants heating temperature ($C \times H$) and stirring speed rpm ($C \times R$) have alleviated the JME yield. Among all, ($C \times M$) with regression coefficient "+4.379" demonstrated the highest effect impact in accelerating the transesterification reaction kinetics for the catalyst loading 2 wt.%–4 wt.% and about 46–65mol./mol.%, Figure 8(b), leading to ">98%" JME yield [67, 68].

3.4.2. Methanol to Oil Ratio (M). Methanol to oil ratio is a primary reactant parameter in the transesterification of VO. The methanol to oil ratio is determined in correlation with a type of VO, catalyst, and other reaction conditions. Figures 8(b), 8(e), 8(f), and 8(g) present the methanol to oil molar ratio with catalyst loading, reaction time, heating temperature, and stirring speed interactions, respectively. The JME yield of ≥98% was reported on to 46°C ± 1°C–56°C ± 1°C operating temperatures. According to the stoichiometric estimations, 30 : 1 mole/mole% methanol to JCO ratio is required [69]; however, in actual esterification experiments a critical methanol to oil ratio which ranges from 30 : 1 to 210 : 1 mol./mol.% was reported to carry out complete reaction, that is, transformation of JCO triglycerides into the JME and glycerin. The linear regression coefficient of methanol to oil ratio (M) in the regression equation (6) "+6.707" refers to its greater influence on transformation reaction process as well as on optimal JME yield%. Although experiments were performed over a range $30 \leq M$ (mol./mol.%) ≤ 70, lower JME yield% results were noted for < 50 mol./mol.% of methanol to oil ratio; this may be due to the insufficient amount of methanol under the reaction conditions set forth, while 50–60 mol./mol.% methanol maximum transformation was achieved relatively compared to the molar ratio which was 60–70 mol./mol.% which indicates keeping the excessive amount of methanol hampers in achieving the reaction equilibrium as well as biodiesel cost economics [62]. The methanol to oil ratio interaction with the stirring speed ($M \times R$) resulted as a positive response. This may be due to increase in the catalytic and transesterification

Table 4: Analysis of variance for optimal JME.

Source	DF	Sum of squares	Adj. sum of squares	Adj. mean of squares	F	P
Blocks	1	99.90	94.69	94.694	14.22	0.0030
Regression	20	1575.49	1575.49	78.775	11.83	<0.0001
Linear	5	632.77	393.59	78.717	11.82	<0.0001
C	1	11.15	0.41	0.405	0.06	0.8100
M	1	328.66	211.45	211.452	31.75	<0.0001
T	1	101.68	92.8	92.800	13.94	0.0030
H	1	187.28	114.13	114.130	17.14	0.0020
R	1	4.00	5.02	5.021	0.75	0.4040
Square	5	902.29	914.24	182.849	27.46	<0.0001
C^2	1	79.02	227.41	227.414	34.15	<0.0001
M^2	1	223.77	351.83	351.831	52.83	<0.0001
T^2	1	301.16	371.36	371.356	55.77	<0.0001
H^2	1	227.14	256.61	256.608	38.53	<0.0001
R^2	1	71.19	78.12	78.117	11.73	0.0060
Interaction	10	40.43	40.43	4.043	0.61	0.7800
$C \times M$	1	6.70	13.55	13.552	2.04	0.1810
$C \times T$	1	0.02	0.23	0.231	0.03	0.8560
$C \times H$	1	3.35	0.65	0.647	0.1	0.7610
$C \times R$	1	0.02	0.04	0.035	0.01	0.9430
$M \times T$	1	3.01	3.01	3.011	0.45	0.5150
$M \times H$	1	9.27	14.18	14.179	2.13	0.1720
$M \times R$	1	0.48	0.38	0.383	0.06	0.8150
$T \times H$	1	2.08	1.84	1.841	0.28	0.6090
$T \times R$	1	12.72	12.72	12.718	1.91	0.1940
$H \times R$	1	2.77	2.77	2.766	0.42	0.5320
Residual error	11	73.25	73.25	6.659		
Lack-of-fit	7	73.22	73.22	10.460	1394.68	<0.0001
Pure error	4	0.03	0.03	0.008		
Total	32	1748.64				

R^2 = 95.81%, R^2_{pred} = 1.97%, and R^2_{adj} = 87.81%.

kinetics as a whole with the stirring speed and hence there is a proportional increase in the % JME yield together with methanol to oil ratio. On the other hand, methanol interactions with parameters heating temperature ($M \times H$: −4.479) and reaction time ($M \times T$: −2.021) were marked as highly negative on the response surface, that is, % JME yield. This is due to the reason that the reactant heating temperatures are close to the methanol boiling point (64.7°C) leading to continuous and rapid evaporation of methanol and hence lesser availability of the methanol for completing the transesterification [70].

3.4.3. Transesterification Reaction Time (T). The requisite duration of reaction time for catalyzed transesterification is governed by factors such as catalyst type, degree of temperature, and also reactants mixing rpm [70, 71]. The effects of transesterification reaction time on JME yield% were investigated in conjunction with catalyst loading, methanol to oil ratio, heating temperature, and stirring speed parameter interactions. The analysis of experimental results is showed graphically in Figures 8(a), 8(e), 8(h), and 8(i) and statistically from (6), the highest significance for interactions of the reaction time and stirring speed ($T \times R$) over interactions ($C \times T$), ($T \times H$), and ($M \times T$) confesses through their regression coefficients "+3.753," "+0.493," "−1.393," and "−2.021," respectively. At the beginning of the transesterification, a passive rate of reaction phase was observed due to the gradual dispersion of methanol into the glycerides in JCO [70, 72]. As the reaction time increases, the amount of triglycerides conversion into ME besides JME yield% was also raised. Normally, across the operational reaction time, the "110 ± 5 min–150 ± 5 min" transesterification iterations results revealed a JME yield of "≥98%." Beyond these reaction duration levels a notable decline in JME yield% was reported. This may be due to the fact that extended reaction timings lead to reversible reactions (1)–(3) which result in continual ester content fall besides soap and diglyceroxide formation [70, 73, 74]. Both methanol to oil ratio and temperature were showing unfavorable interactions with reaction time. Hence, an appropriate reaction time was maintained.

3.4.4. Heating Temperature (H). The transesterification reaction kinetics was significantly affected by the reactants heating temperature [3]. Figures 8(c), 8(f), 8(h), and 8(j) present

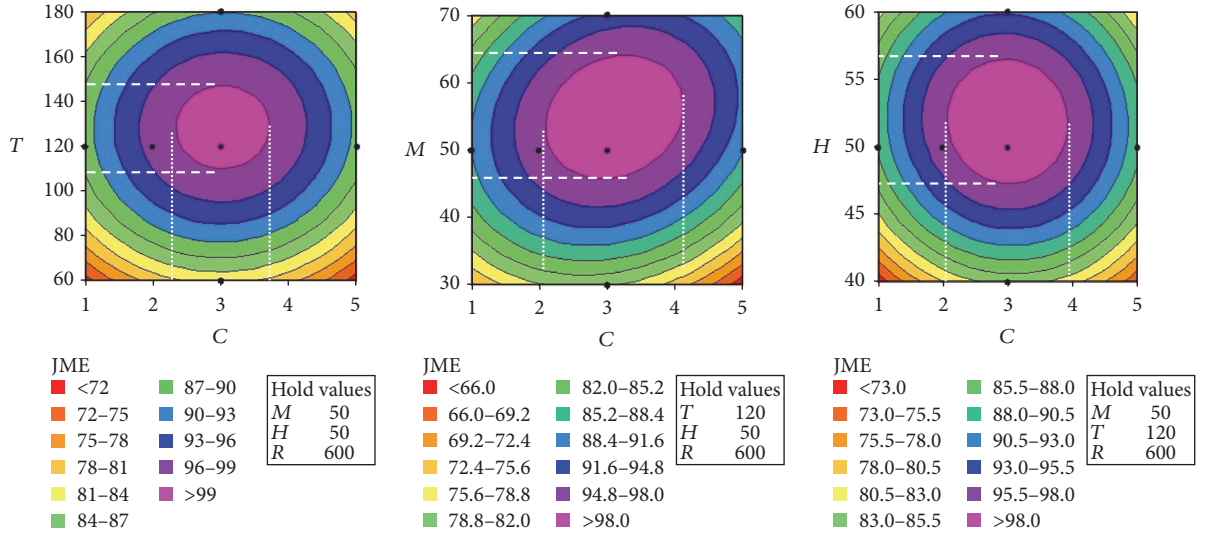

(a) Reaction time and catalyst concentration ($T \times C$)

(b) Methanol to oil ratio and catalyst concentration ($M \times C$)

(c) Heating temperature and catalyst concentration ($H \times C$)

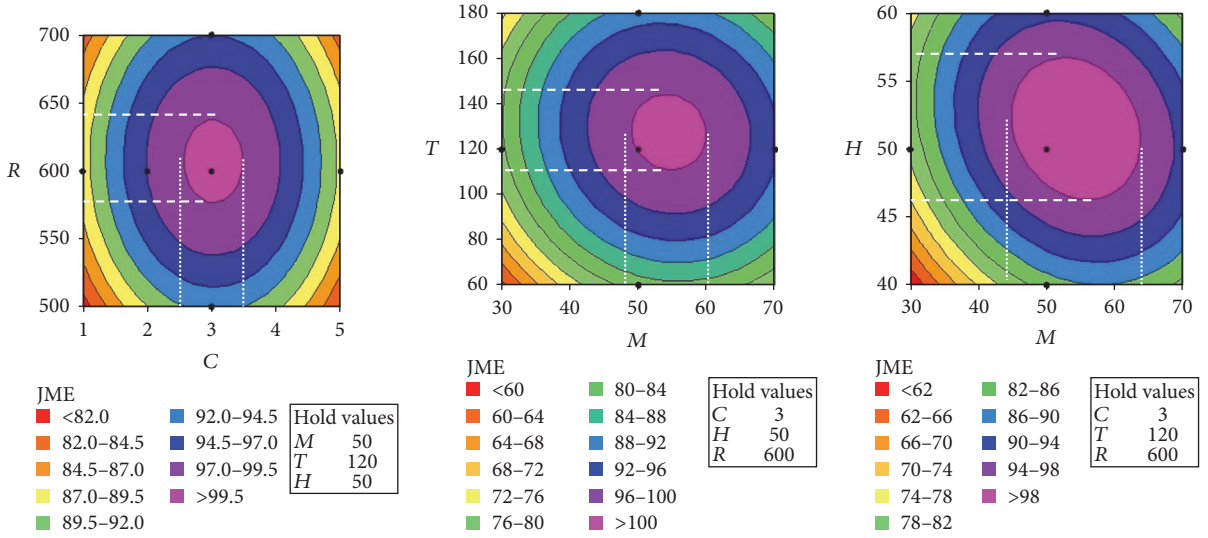

(d) Stirring speed and catalyst concentration ($R \times C$)

(e) Reaction time and methanol to oil ratio ($T \times M$)

(f) Heating temperature and methanol to oil ratio ($H \times M$)

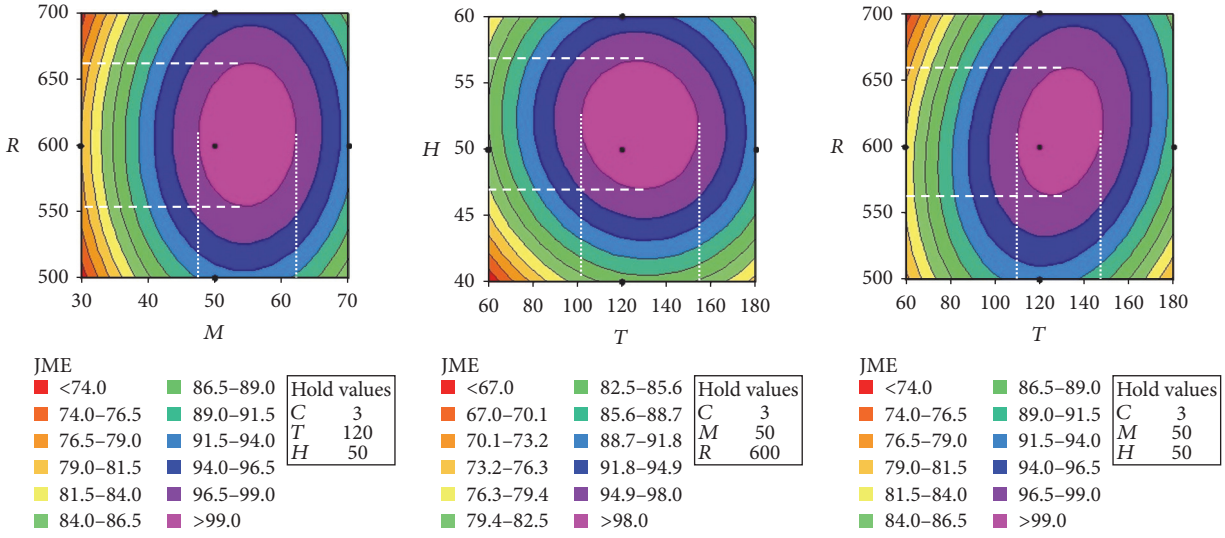

(g) Stirring speed and methanol to oil ratio ($R \times M$)

(h) Heating temperature and reaction time ($H \times T$)

(i) Stirring speed and reaction time ($R \times T$)

Figure 8: Continued.

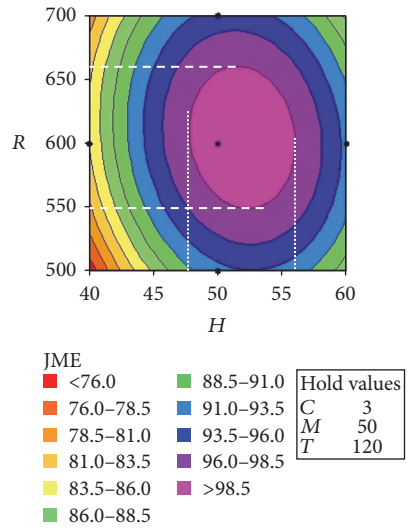

(j) Stirring speed and heating temperature ($R \times H$)

Figure 8: Contour plots showing transesterification parametric interactions impact on JME yield.

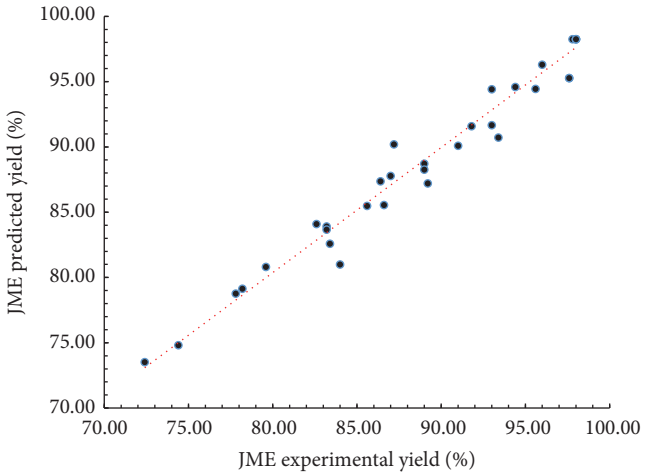

Figure 9: Comparative graph of JME predicted and experimental yields.

the interactions of heating temperature over 40°C–60°C with the catalyst loading, methanol molar ratio, reaction time, and stirring speed. The study of temperature effect is very crucial since a JME yield of "≥98%" was reported on to 46°C ± 1°C–56°C ± 1°C. Both higher and lower temperature ranges showed distinct negative impacts on the reaction process. The use of heterogeneous catalysts suffers from their poor rates of reaction compared to homogeneous catalysts; however, higher reaction pressures and temperatures can contribute in accelerating the reaction rate [75]. The reaction time gets shorter with higher temperatures and accelerates the rate of reaction but then rises the viscosity of reactants and reduces methyl esters conversion [3, 76]. Also, the increase in reaction temperature eventually results in rapid evaporation of methanol which can greatly promotes saponification besides leading to side reactions and soap formation [3, 76]. Despite a proper water cooling condenser attachment, if the operating temperature approaches close to boiling point of methanol, 64.7°C, evaporation of methanol accelerates [70, 72]. This effect was evident from the experimental results tabulated in Table 2. Likewise, the interaction ($M \times H$) bears the relatively highest negative regression coefficient of "−4.479" besides the fact that other interactions include ($C \times H$), ($T \times H$), and ($H \times R$). All these predominantly indicate that an increase in heating temperature does not appreciate the JME yield rather than reducing the whole reaction activity. Therefore, the heating temperature ranges are lower than methanol boiling point which minimizes its exponential vaporization and allows maintaining sufficient methanol levels during the transesterification.

3.4.5. Stirring Speed rpm (R). Stirring speed of reactants is one of the key reaction parameters in the biodiesel production through heterogeneous catalyzed transesterification process [3, 44, 77]. In Figures 8(d), 8(g), 8(i), and 8(j) the stirring speed interaction effects on JME yield together with the catalyst loading, methanol molar ratio, reaction time, and heating temperature were plotted. From the graphical results JME yield of "≥99 ± 0.5%" can be seen. Besides, the stirring speed interactions on the reaction time ($T \times R$) and methanol to oil ratio ($M \times R$) were comparably significant, with regression coefficients "+3.759" and "+0.721" as noted from (6). Even though the other two interactions ($C \times R$) and ($H \times R$) are indicated with negative regression coefficients, Figures 8(d) and 8(j) contour plots demonstrate a JME yield of "99.5%" and "98.5%," respectively. This emphasizes that a stirring speed is a productive reaction parameter in achieving a maximum JME yield.

3.5. Optimization of Reaction Parameters and Results Validation. Optimal % JME yield was obtained by comprehensive integration analysis of linear and interaction impacts of all

Table 5: Predicted JME yield % data sets validation at optimal conditions with experimental results.

Data set	Optimal condition					JME yield (%)	
	Catalyst loading (wt.%)	Methanol to oil ratio (mol./mol.%)	Reaction time (min)	Heating temperature (°C)	Stirring speed (rpm)	Predicted	Experimental
Set-1	2.95	54.30	157.44	50.43	621.92	98.02	97.04
Set-2	3.07	54.29	157.30	50.43	624.79	98.14	97.26
Set-3	3.10	54.72	157.66	50.37	622.11	98.03	97.05
Set-4	3.29	54.31	156.41	50.45	627.48	98.25	97.37
Set-5	*3.22*	*53.23*	*138.78*	*51.98*	*561.18*	*98.89*	*98.00*
Set-6	3.09	55.28	106.53	50.92	631.88	98.42	97.53
Set-7	3.15	54.65	157.58	50.38	622.81	98.05	97.85
Set-8	*3.29*	*53.42*	*137.73*	*51.97*	*560.38*	*98.80*	*97.92*
Set-9	*3.10*	*54.24*	*127.87*	*51.31*	*611.11*	*99.20*	*98.80*
Set-10	*2.96*	*55.96*	*128.71*	*51.31*	*611.11*	*99.41*	*98.62*

Table 6: Fatty acid composition analysis of JCO.

Fatty acid	JCO (%)
Palmitic acid (C16:0)	14.35
Palmitoleic acid (C16:1)	1.52
Stearic acid (C18:0)	7.02
Oleic acid (C18:1)	43.15
Linoleic acid (C18:2)	33.92
Linolenic acid (C18:3)	0.04

five reaction parameters. The comparative analysis of both statistical and experimental results along with the interaction contour plots reveals a significant effect of a reaction parameter at a specific parameter levels. However, the minimum levels of any parameter were not intended to obtain optimal JME yield. The optimization of transesterification reaction parameters was carried out using a response surface optimizer tool and the results were validated for ten sets through confirmatory experiments successively. Data validation for ten sets together with the predicted and experimental results were tabulated as listed in Table 5. Among the ten validation test results 98.80% of JME yield was noted at optimal conditions C (3.10 wt.%), M (54.24 mol./mol.%), T (127.87 min), H (51.31°C), and R (612 rpm) for the data set-9. A similar result with a simple variation of "−0.18%" JME yield was achieved for data set-10. The parametric optimal results are ascertained with previously published results [22–24, 49]. Further, the Razor shell CaO performance as a catalyst in converting the triglycerides of JCO to JME is comparable with literature reports by Tan et al. [14], Margaretha et al. [19], De Sousa et al. [21], Roschat et al. [50], McDevitt and Baun [51], Nasrazadani and Eureste [52], Zaki et al. [53], Mirghiasi et al. [54], Teo et al. [55], and Chen et al. [56].

3.6. Analysis of Razor Shell CaO Reusability, Leaching Analysis, and Transesterification with Reference Catalyst. The Razor shell CaO catalyst reusability transesterification experiments of the pretreated JCO and methanol were carried out with optimal conditions of C (3.10 wt.%), M (54.24 mol./mol.%), T (127.87 min), H (51.31°C), and R (612 rpm) as obtained and under similar experimental protocols for five successive catalyst reuse cycles. Figure 10(a) shows variations in JME yield from five successive reuse cycles 97.62%, 95.75%, 91.52%, 84.33%, and 76.40%, respectively. The SEM monograms (Figures 10(b)–10(f)) depict changes in surface morphology of reused Razor shell CaO catalyst over five cycles successively. The reduction in JME yield may be due to the gradual loss of active sites on the catalyst surface, particle agglomerations with other reactant molecules, and/or calcium catalyst leaching to the biodiesel [13, 14]. An averaNge JME yield of 93.6% was noted up to the 4th catalyst reuse cycle. However, during the 5th catalyst reuse cycle JME yield was 76.40%, which is remarkably less by 7.93% from the 4th reuse cycle. Besides, the leaching of Razor shell CaO catalyst was carried out successively using AAS for measuring calcium ion (Ca^{2+}) leached to JME. The test results indicate Ca^{2+} dispersion range of 1.43 ppm ± 0.11 to 4.25 ppm ± 0.21 during the 1st and 4th reuse cycles, which indicate compliance with EN14214 fuel standards. However, from the 5th reuse cycle, Ca^{2+} of 6.67 ppm ± 1.09 was reported and subsequently dropped in JME yield besides increased leaching. Hence, it can be concluded that the Razor shell CaO is stable for four reuse cycles. Transesterification of JCO using lab grade CaO together with catalyst reuse tests was conducted at optimal conditions as obtained. Results of % JME yield using from both Razor shell CaO and lab grade CaO are shown in Figure 10. The JME yield achieved from Razor shell CaO is higher besides good catalytic performance over its reusability. Moreover, the JME yield obtained from present investigations is comparably higher than other researchers, Tan et al. [14], reported. This variation in JME yield can be attributed to the higher catalyst surface area, particle size, and pore volume of Razor shell CaO compared to catalysts used by Tan et al. [14].

3.7. JME Fuel Properties Analysis. The JME fuel property test results such as density at 15°C, calorific value, flash point, cetane value, specific gravity at 15°C, viscosity at 40°C, water content, ash content, acid value, monoglyceride,

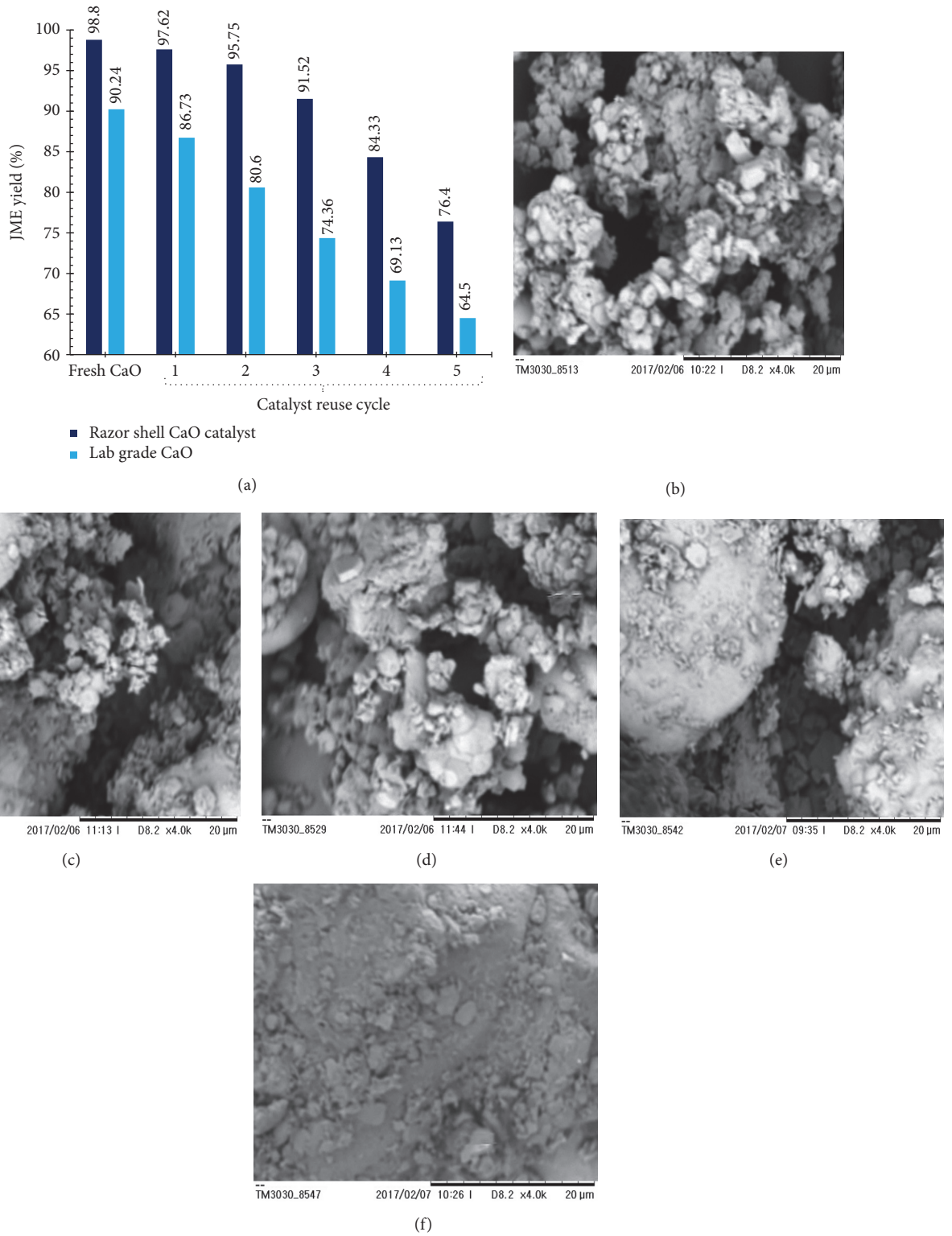

Figure 10: (a) JME yield study over Razor shell CaO and lab grade CaO catalysts reuse at optimal transesterification reaction conditions. (b–f) SEM images of Razor shell CaO catalyst presenting catalyst surface structure variations after reuse.

Table 7: JME fuel properties.

Fuel property (units)	JME	EN 14214 limit
Density at 15°C (kg/m^3)	883	860–900
Calorific value (MJ/kg)	36.284	—
Flash point (°C)	167	>101
Cetane value	52	>47
Specific gravity at 15°C (g/ml)	0.878	0.86–0.90
viscosity at 40°C (mm^2/s)	4.22	3.5–5.0
Water content (Wt%)	0.044	<0.05
Ash content (g/100 g)	<0.01	<0.01
Acid value (Mg KOH/g)	0.28	<0.5
Monoglyceride (Wt%)	0.311	<0.80
Diglyceride (Wt%)	0.033	<0.20
Triglyceride (Wt%)	0	<0.20
Free glycerin (Wt%)	0	<0.02
Total ester (Wt%)	99.11	>96.5
Total glycerin (Wt%)	0.03	<0.25

diglyceride, triglyceride, free glycerine, total ester content, and total glycerine contents are summarized in Table 7. The results are compliance with the European biodiesel standard EN14214; thus JME indicates its suitability as a green biodiesel source.

4. Conclusions

Synthesis of heterogeneous CaO catalyst using Razor shells conformed by spectral characterization results of FTIR, SEM, XRD, BET&BJH, and PSA with a crystalline size of 87.2 nm, S_{BET} of 92.63 m^2/g, pore diameters of 37.311 nm, and pore volume of 0.613 cc/g which signifies CaO as an active catalyst. CaO was derived using a green synthesis protocol "calcination-hydro aeration-dehydration." The catalyst yielded an optimal Jatropha methyl ester (JME) of 98.80% via two-step transesterification of *Jatropha curcas* oil (JCO) at C (3.10 wt.%), M (54.24 mol./mol.%), T (127.87 min), H (51.31°C), and R (612 rpm). The reaction kinetics and JME yield optimization were investigated utilizing a five-factor-five-level, two-block, half factorial, central composite design (CCD) based response surface method (RSM) design. The atomic absorption spectroscopic characterization of JME showed minimal leaching of calcium to JME until catalyst of 4th reuse cycle. The amount of Ca leaching increases for each type of reuse and subsequently reduces JME yield. The fuel properties tested according to biodiesel standards EN 14214 comply with JME's suitability as a green biodiesel and offers sustainable benefits.

Conflicts of Interest

The authors declare that there are no conflicts of interest regarding the publishing of this paper.

Acknowledgments

The authors would like to thank Faculty of Engineering, UNIMAS, and all the staff members for providing research facilities and continuous support during this work. The first author, A. N. R. Reddy, would greatly acknowledge and express his highest gratitude to Ministry of Higher Education, Malaysia, for awarding prestigious Malaysian International Scholarship (MIS) 2015; KPT.B.600-4/1/12 (60).

References

[1] G. B. Asheim, WPS1302, The World Bank, Washington, DC, USA, 1994, http://www-wds.worldbank.org/servlet/WDSContentServer/WDSP/IB/1994/05/01/000009265_3970716141011/Rendered/PDF/multi0page.pdf.

[2] US-EPA, "RFS2: EPA-420-R-10-003, Washington DC, USA," 2010 http://www3.epa.gov/otaq/renewablefuels/420r10003.pdf.

[3] J. Qian, H. Shi, and Z. Yun, "Preparation of biodiesel from *Jatropha curcas* L. oil produced by two-phase solvent extraction," *Bioresource Technology*, vol. 101, no. 18, pp. 7025–7031, 2010.

[4] L. C. Meher, C. P. Churamani, M. Arif, Z. Ahmed, and S. N. Naik, "Jatropha curcas as a renewable source for bio-fuels—a review," *Renewable and Sustainable Energy Reviews*, vol. 26, pp. 397–407, 2013.

[5] I. Noshadi, N. A. S. Amin, and R. S. Parnas, "Continuous production of biodiesel from waste cooking oil in a reactive distillation column catalyzed by solid heteropolyacid: optimization using response surface methodology (RSM)," *Fuel*, vol. 94, pp. 156–164, 2012.

[6] E. F. Aransiola, T. V. Ojumu, O. O. Oyekola, T. F. Madzimbamuto, and D. I. O. Ikhu-Omoregbe, "A review of current technology for biodiesel production: state of the art," *Biomass and Bioenergy*, vol. 61, pp. 276–297, 2014.

[7] J. M. Marchetti, V. U. Miguel, and A. F. Errazu, "Possible methods for biodiesel production," *Renewable and Sustainable Energy Reviews*, vol. 11, no. 6, pp. 1300–1311, 2007.

[8] S. H. Teo, Y. H. Taufiq-Yap, U. Rashid, and A. Islam, "Hydrothermal effect on synthesis, characterization and catalytic properties of calcium methoxide for biodiesel production from crude *Jatropha curcas*," *RSC Advances*, vol. 5, no. 6, pp. 4266–4276, 2015.

[9] E. W. Thiele, "Relation between catalytic activity and size of particle," *Industrial & Engineering Chemistry*, vol. 31, no. 7, pp. 916–920, 1939.

[10] A. Buasri, N. Chaiyut, V. Loryuenyong, P. Worawanitchaphong, and S. Trongyong, "Calcium oxide derived from waste shells of mussel, cockle, and scallop as the heterogeneous catalyst for biodiesel production," *The Scientific World Journal*, vol. 2013, Article ID 460923, 7 pages, 2013.

[11] H. A. Choudhury, P. P. Goswami, R. S. Malani, and V. S. Moholkar, "Ultrasonic biodiesel synthesis from crude Jatropha curcas oil with heterogeneous base catalyst: mechanistic insight and statistical optimization," *Ultrasonics Sonochemistry*, vol. 21, no. 3, pp. 1050–1064, 2014.

[12] S. H. Teo, U. Rashid, and Y. H. Taufiq-Yap, "Biodiesel production from crude Jatropha Curcas oil using calcium based mixed oxide catalysts," *Fuel*, vol. 136, pp. 244–252, 2014.

[13] Y. H. Taufiq-Yap, H. V. Lee, M. Z. Hussein, and R. Yunus, "Calcium-based mixed oxide catalysts for methanolysis of *Jatropha curcas* oil to biodiesel," *Biomass and Bioenergy*, vol. 35, no. 2, pp. 827–834, 2011.

[14] Y. H. Tan, M. O. Abdullah, C. Nolasco-Hipolito, and Y. H. Taufiq-Yap, "Waste ostrich- and chicken-eggshells as heterogeneous base catalyst for biodiesel production from used cooking oil: catalyst characterization and biodiesel yield performance," *Applied Energy*, vol. 160, pp. 58–70, 2015.

[15] A. Kawashima, K. Matsubara, and K. Honda, "Acceleration of catalytic activity of calcium oxide for biodiesel production," *Bioresource Technology*, vol. 100, no. 2, pp. 696–700, 2009.

[16] R. Shan, C. Zhao, P. Lv, H. Yuan, and J. Yao, "Catalytic applications of calcium rich waste materials for biodiesel: current state and perspectives," *Energy Conversion and Management*, vol. 127, pp. 273–283, 2016.

[17] M. Mohamed, N. A. Rashidi, S. Yusup, L. K. Teong, U. Rashid, and R. M. Ali, "Effects of experimental variables on conversion of cockle shell to calcium oxide using thermal gravimetric analysis," *Journal of Cleaner Production*, vol. 37, pp. 394–397, 2012.

[18] S. Nurdin, "Activated *Paphia undulate* shells waste (APSW): a cost-effective catalyst for biodiesel synthesis from *Rubber* and *Jatropha curcas* seeds oil (RSOME & JSOME)," *International Journal of Chemical Engineering and Applications*, vol. 5, no. 6, pp. 483–488, 2014.

[19] Y. Y. Margaretha, H. S. Prastyo, A. Ayucitra, and S. Ismadji, "Calcium oxide from pomacea sp. shell as a catalyst for biodiesel production," *International Journal of Energy and Environmental Engineering*, vol. 3, no. 1, article 33, 2012.

[20] K. N. Islam, M. Z. B. A. Bakar, M. E. Ali et al., "A novel method for the synthesis of calcium carbonate (aragonite) nanoparticles from cockle shells," *Powder Technology*, vol. 235, pp. 70–75, 2013.

[21] F. P. De Sousa, G. P. Dos Reis, C. C. Cardoso, W. N. Mussel, and V. M. D. Pasa, "Performance of CaO from different sources as a catalyst precursor in soybean oil transesterification: kinetics and leaching evaluation," *Journal of Environmental Chemical Engineering*, vol. 4, no. 2, pp. 1970–1977, 2016.

[22] A. Okullo, A. K. Temu, J. W. Ntalikwa, and P. Ogwok, "Optimization of biodiesel production from *Jatropha* oil," *International Journal of Engineering Research in Africa*, vol. 3, pp. 62–73, 2010.

[23] P. Goyal, M. P. Sharma, and S. Jain, "Optimization of esterification and transesterification of high FFA Jatropha curcas oil using response surface methodology," *Journal of Petroleum Science and Engineering*, vol. 1, no. 3, pp. 36–43, 2012.

[24] U. Rashid, F. Anwar, B. R. Moser, and S. Ashraf, "Production of sunflower oil methyl esters by optimized alkali-catalyzed methanolysis," *Biomass and Bioenergy*, vol. 32, no. 12, pp. 1202–1205, 2008.

[25] R. Anr, A. A. Saleh, M. S. Islam, S. Hamdan, and M. A. Maleque, "Biodiesel production from crude *Jatropha* oil using a highly active heterogeneous nanocatalyst by optimizing transesterification reaction parameters," *Energy and Fuels*, vol. 30, no. 1, pp. 334–343, 2016.

[26] S. Pradhan, C. S. Madankar, P. Mohanty, and S. N. Naik, "Optimization of reactive extraction of castor seed to produce biodiesel using response surface methodology," *Fuel*, vol. 97, pp. 848–855, 2012.

[27] A. Kumar Tiwari, A. Kumar, and H. Raheman, "Biodiesel production from jatropha oil (Jatropha curcas) with high free fatty acids: an optimized process," *Biomass and Bioenergy*, vol. 31, no. 8, pp. 569–575, 2007.

[28] G. Vicente, A. Coteron, M. Martinez, and J. Aracil, "Application of the factorial design of experiments and response surface methodology to optimize biodiesel production," *Industrial Crops and Products*, vol. 8, no. 1, pp. 29–35, 1998.

[29] S. Dhingra, K. K. Dubey, and G. Bhushan, "Enhancement in Jatropha-based biodiesel yield by process optimisation using design of experiment approach," *International Journal of Sustainable Energy*, vol. 33, no. 4, pp. 842–853, 2014.

[30] S. Dhingra, G. Bhushan, and K. K. Dubey, "Development of a combined approach for improvement and optimization of karanja biodiesel using response surface methodology and genetic algorithm," *Frontiers in Energy*, vol. 7, no. 4, pp. 495–505, 2013.

[31] D. Kanakaraju, C. Jios, and S. M. Long, "Heavy metal concentrations in the Razor Clams (*Solen* spp) from Muara Tebas, Sarawak," *Malaysian Journal of Analytical Sciences*, vol. 12, pp. 53–58, 2008.

[32] S. Akmar and K. Ab. Rahim, "Razor Clam (*Solen* spp.) fishery in Sarawak, Malaysia," *Kuroshio Science*, vol. 5, no. 1, pp. 87–94, 2011.

[33] M. F. Hossen, S. Hamdan, and M. R. Rahman, "Review on the risk assessment of heavy metals in Malaysian clams," *The Scientific World Journal*, vol. 2015, Article ID 905497, 7 pages, 2015.

[34] K. N. Islam, M. Z. B. A. Bakar, M. M. Noordin, M. Z. Bin Hussein, N. S. B. A. Rahman, and M. E. Ali, "Characterisation of calcium carbonate and its polymorphs from cockle shells (*Anadara granosa*)," *Powder Technology*, vol. 213, no. 1, pp. 188–191, 2011.

[35] A. N. R. Reddy, A. A. Saleh, S. Islam, and S. Hamdan, "Optimization of transesterification parameters for optimal biodiesel yield from Crude Jatropha oil using a newly synthesized seashell catalyst," *Journal of Engineering Science and Technology*, In press.

[36] A. N. R. Reddy, A. Saleh, M. S. Islam, and S. Hamdan, "Active heterogeneous CaO catalyst synthesis from *Anadara granosa* (Kerang) seashells for Jatropha biodiesel production," *MATEC Web of Conferences*, vol. 87, Article ID 02008, 6 pages, 2017.

[37] S. Ismail, A. S. Ahmed, R. Anr, and S. Hamdan, "Biodiesel production from castor oil by using calcium oxide derived from mud clam shell," *Journal of Renewable Energy*, vol. 2016, Article ID 5274917, 8 pages, 2016.

[38] A. N. R. Reddy, A. A. Saleh, M. D. S. Islam, and S. Hamdan, "Methanolysis of Crude Jatropha oil using heterogeneous catalyst from the seashells and eggshells as green biodiesel," *ASEAN*

Journal on Science and Technology for Development, vol. 32, no. 1, pp. 16–30, 2015.

[39] X. Deng, Z. Fang, and Y. H. Liu, "Ultrasonic transesterification of Jatropha curcas L. oil to biodiesel by a two-step process," *Energy Conversion and Management*, vol. 51, no. 12, pp. 2802–2807, 2010.

[40] S. Niju, K. M. Meera Sheriffa Begum, and N. Anantharaman, "Enhancement of biodiesel synthesis over highly active CaO derived from natural white bivalve clam shell," *Arabian Journal of Chemistry*, vol. 9, pp. 633–639, 2016.

[41] S. Niju, M. S. Begum, and N. Anantharaman, "Modification of egg shell and its application in biodiesel production," *Journal of Saudi Chemical Society*, vol. 18, no. 5, pp. 702–706, 2014.

[42] B. Yoosuk, P. Udomsap, B. Puttasawat, and P. Krasae, "Improving transesterification acitvity of CaO with hydration technique," *Bioresource Technology*, vol. 101, no. 10, pp. 3784–3786, 2010.

[43] A. Bazargan, M. D. Kostić, O. S. Stamenković, V. B. Veljković, and G. McKay, "A calcium oxide-based catalyst derived from palm kernel shell gasification residues for biodiesel production," *Fuel*, vol. 150, pp. 519–525, 2015.

[44] P.-L. Boey, G. P. Maniam, and S. A. Hamid, "Biodiesel production via transesterification of palm olein using waste mud crab (Scylla serrata) shell as a heterogeneous catalyst," *Bioresource Technology*, vol. 100, no. 24, pp. 6362–6368, 2009.

[45] A. K. Endalew, Y. Kiros, and R. Zanzi, "Heterogeneous catalysis for biodiesel production from Jatropha curcas oil (JCO)," *Energy*, vol. 36, no. 5, pp. 2693–2700, 2011.

[46] H. V. Lee, J. C. Juan, N. F. Binti Abdullah, R. Nizah MF, and Y. H. Taufiq-Yap, "Heterogeneous base catalysts for edible palm and non-edible Jatropha-based biodiesel production," *Chemistry Central Journal*, vol. 8, no. 1, article 30, 2014.

[47] X. Deng, Z. Fang, Y.-H. Liu, and C.-L. Yu, "Production of biodiesel from Jatropha oil catalyzed by nanosized solid basic catalyst," *Energy*, vol. 36, no. 2, pp. 777–784, 2011.

[48] H. J. Berchmans and S. Hirata, "Biodiesel production from crude Jatropha curcas L. seed oil with a high content of free fatty acids," *Bioresource Technology*, vol. 99, no. 6, pp. 1716–1721, 2008.

[49] D. Vujicic, D. Comic, A. Zarubica, R. Micic, and G. Boskovic, "Kinetics of biodiesel synthesis from sunflower oil over CaO heterogeneous catalyst," *Fuel*, vol. 89, no. 8, pp. 2054–2061, 2010.

[50] W. Roschat, T. Siritanon, T. Kaewpuang, B. Yoosuk, and V. Promarak, "Economical and green biodiesel production process using river snail shells-derived heterogeneous catalyst and co-solvent method," *Bioresource Technology*, vol. 209, pp. 343–350, 2016.

[51] N. T. McDevitt and W. L. Baun, "Infrared absorption study of metal oxides in the low frequency region (700-240 cm-1)," *Spectrochimica Acta*, vol. 20, no. 5, pp. 799–808, 1964.

[52] S. Nasrazadani and E. Eureste, "Application of FTIR for Quantitative Lime Analysis," Denton Texas, 2008 https://www.ntis.gov/.

[53] M. I. Zaki, H. Knözinger, B. Tesche, and G. A. H. Mekhemer, "Influence of phosphonation and phosphation on surface acid-base and morphological properties of CaO as investigated by in situ FTIR spectroscopy and electron microscopy," *Journal of Colloid and Interface Science*, vol. 303, no. 1, pp. 9–17, 2006.

[54] Z. Mirghiasi, F. Bakhtiari, E. Darezereshki, and E. Esmaeilzadeh, "Preparation and characterization of CaO nanoparticles from Ca(OH)2 by direct thermal decomposition method," *Journal of Industrial and Engineering Chemistry*, vol. 20, no. 1, pp. 113–117, 2014.

[55] S. H. Teo, A. Islam, F. L. Ng, and Y. H. Taufiq-Yap, "Biodiesel synthesis from photoautotrophic cultivated oleoginous microalgae using a sand dollar catalyst," *RSC Advances*, vol. 5, no. 58, pp. 47140–47152, 2015.

[56] G. Chen, R. Shan, J. Shi, and B. Yan, "Ultrasonic-assisted production of biodiesel from transesterification of palm oil over ostrich eggshell-derived CaO catalysts," *Bioresource Technology*, vol. 171, pp. 428–432, 2014.

[57] Y. Ren, Z. Ma, and P. G. Bruce, "Ordered mesoporous metal oxides: synthesis and applications," *Chemical Society Reviews*, vol. 41, no. 14, p. 4909, 2012.

[58] Ž. Kesić, I. Lukić, D. Brkić et al., "Mechanochemical preparation and characterization of CaO•ZnO used as catalyst for biodiesel synthesis," *Applied Catalysis A: General*, vol. 427-428, pp. 58–65, 2012.

[59] E. W. Thiele, "Relation between catalytic activity and size of particle," *Industrial & Engineering Chemistry*, vol. 31, no. 7, pp. 916–920, 1939.

[60] D. C. Montgomery, *Design and Analysis of Experiments*, John Wiley & Sons, 8th edition, 2012, https://books.google.com.my/books?id=XQAcAAAAQBAJ.

[61] H. Ceylan, S. Kubilay, N. Aktas, and N. Sahiner, "An approach for prediction of optimum reaction conditions for laccase-catalyzed bio-transformation of 1-naphthol by response surface methodology (RSM)," *Bioresource Technology*, vol. 99, no. 6, pp. 2025–2031, 2008.

[62] P. Verma, M. P. Sharma, and G. Dwivedi, "Impact of alcohol on biodiesel production and properties," *Renewable and Sustainable Energy Reviews*, vol. 56, pp. 319–333, 2016.

[63] G. Joshi, D. S. Rawat, B. Y. Lamba et al., "Transesterification of Jatropha and Karanja oils by using waste egg shell derived calcium based mixed metal oxides," *Energy Conversion and Management*, vol. 96, pp. 258–267, 2015.

[64] A. P. S. Chouhan and A. K. Sarma, "Modern heterogeneous catalysts for biodiesel production: a comprehensive review," *Renewable and Sustainable Energy Reviews*, vol. 15, no. 9, pp. 4378–4399, 2011.

[65] M. Sánchez, F. Bergamin, E. Peña, M. Martínez, and J. Aracil, "A comparative study of the production of esters from *Jatropha* oil using different short-chain alcohols: optimization and characterization," *Fuel*, vol. 143, pp. 183–188, 2015.

[66] G. Knothe, "Analyzing biodiesel: standards and other methods," *Journal of the American Oil Chemists' Society*, vol. 83, no. 10, pp. 823–833, 2006.

[67] K. Boonmee, S. Chuntranuluck, V. Punsuvon, and P. Silayoi, "Optimization of biodiesel production from Jatropha oil (*Jatropha curcas* L.) using response surface methodology," *Journal of Sustainable Energy & Environment*, vol. 299, pp. 290–299, 2010.

[68] R. Sathish Kumar, K. Sureshkumar, and R. Velraj, "Optimization of biodiesel production from Manilkara zapota (L.) seed oil using Taguchi method," *Fuel*, vol. 140, pp. 90–96, 2015.

[69] F. Ma and M. A. Hanna, "Biodiesel production: a review," *Bioresource Technology*, vol. 70, no. 1, pp. 1–15, 1999.

[70] D. Y. C. Leung, X. Wu, and M. K. H. Leung, "A review on biodiesel production using catalyzed transesterification," *Applied Energy*, vol. 87, no. 4, pp. 1083–1095, 2010.

[71] D. Y. C. Leung and Y. Guo, "Transesterification of neat and used frying oil: optimization for biodiesel production," *Fuel Processing Technology*, vol. 87, no. 10, pp. 883–890, 2006.

[72] B. Freedman, E. H. Pryde, and T. L. Mounts, "Variables affecting the yields of fatty esters from transesterified vegetable oils,"

Journal of the American Oil Chemists Society, vol. 61, no. 10, pp. 1638–1643, 1984.

[73] K. Prasertsit, P. Phoosakul, and S. Sukmanee, "Use of calcium oxide in palm oil methyl ester production," *Songklanakarin Journal of Science and Technology*, vol. 36, no. 2, pp. 195–200, 2014.

[74] M. Kouzu, T. Kasuno, M. Tajika, S. Yamanaka, and J. Hidaka, "Active phase of calcium oxide used as solid base catalyst for transesterification of soybean oil with refluxing methanol," *Applied Catalysis A: General*, vol. 334, no. 1-2, pp. 357–365, 2008.

[75] A. C. Alba-Rubio, M. L. Alonso Castillo, M. C. G. Albuquerque, R. Mariscal, C. L. Cavalcante Jr., and M. L. Granados, "A new and efficient procedure for removing calcium soaps in biodiesel obtained using CaO as a heterogeneous catalyst," *Fuel*, vol. 95, pp. 464–470, 2012.

[76] S. M. Hailegiorgis, S. Mahadzir, and D. Subbarao, "Parametric study and optimization of in situ transesterification of *Jatropha curcas* L assisted by benzyltrimethylammonium hydroxide as a phase transfer catalyst via response surface methodology," *Biomass and Bioenergy*, vol. 49, pp. 63–73, 2013.

[77] P. K. Roy, S. Datta, S. Nandi, and F. Al Basir, "Effect of mass transfer kinetics for maximum production of biodiesel from Jatropha Curcas oil: a mathematical approach," *Fuel*, vol. 134, pp. 39–44, 2014.